Analytical neutrino structure in Einstein-de Sitter

Analytisk neutrino struktur i Einstein-de Sitter

Erik Holm Steenberg
201804655

Master's Thesis in Physics
June 2023

Supervisors: Thomas Tram & Steen Hannested

Department of Physics and Astronomy
Aarhus University

Colophon

Analytical neutrino structure in Einstein-de Sitter

— Analytisk neutrino struktur i Einstein-de Sitter

Master's thesis by Erik Holm Steenberg. Written under supervision by Prof. Steen Hannested & Assoc. Prof. Thomas Tram, Department of Physics and Astronomy, Aarhus University.

Typeset by the author with LaTeX and the memoir document class, using Linux Libertine and Linux Biolinum 12.0/14.5pt.

Printed at Aarhus University

Abstract (English)

The goal of this thesis is to present a new equation that can describe the neutrino density perturbation. The equation is derived by using the method of an effective sound speed and assuming a matter dominated universe (the Einstein-de Sitter model). Expansions of this new equation are also presented. The equation and numerical solutions, solved in python, are compared with the "Cosmic Linear Anisotropy Solving System" code CLASS. The equation is in agreement with the numerical solutions by CLASS, although we find that the value of the effective sound speed based on [1] may be a bit too high for certain scales. Based on the expansions, we also conclude that the effective sound speed term remains relevant for a very long time, unlike what we initially believed.

Resumé (Dansk)

Målet med dette speciale er at præsentere en ny ligning, der kan beskrive neutrinodensitetsperturbationer. Ligningen er udledt ved bruge af en effektiv lydhastighed og under antagelse af et stofdomineret univers (Einstein-de Sitter-modellen). Rækkeudviklinger af denne nye ligning præsenteres også. Ligningen og numeriske løsninger, løst i python, sammenlignes med koden "Cosmic Linear Anisotropy Solving System"CLASS. Ligningen er i overensstemmelse med de numeriske løsninger fra CLASS, selvom vi finder at værdien af den effektive lydhastighed baseret på [1] kan være lidt for høj for visse skalaer. Baseret på rækkeudviklingerne konkluderer vi også, at den effektive lydhastighedsperiode forbliver relevant i meget lang tid, i modsætning til hvad vi oprindeligt troede.

Acknowledgments

I would like to thank my supervisors, Steen Hannested and Thomas Tram for guiding me through this thesis. I would also like to thank Ph.D. students Emil Brinch Holm and Andreas Nygaard Hansen for their help in explaining my many questions and proofreading the first draft of this thesis. Additionally, I would like to thank Christiane Rahbeck, Hans B. Dein, Jacob B. Thomsen, Martin C. Østerlund, and Camilla T. Sørensen for their support and for creating a fun working environment.

Contents

Introduction

The formation and evolution of cosmic structures, such as galaxies and galaxy clusters, are of high importance in modern cosmology. Understanding the mechanisms driving the growth of these structures is crucial to understanding the mysteries of the universe. Over cosmic timescales, tiny density fluctuations in the early universe have undergone gravitational collapse, leading to the emergence of the cosmic web. Many factors have influenced the structure formation of the universe, including the gravitational interactions between different components of the universe, such as dark matter, baryonic matter, radiation, and neutrinos[2]. Neutrinos, which are electrically neutral and weakly interacting elementary particles, are the focus of this thesis. While they were once believed to be massless, through neutrino oscillation experiments it has been established that neutrinos possess small, non-zero masses[3]. This has profound implications for our understanding of neutrino physics and their cosmological implications. With a mass and weak interactions, the neutrinos may thus be seen as a form of hot dark matter. To understand the behavior of neutrinos within the framework of structure formation, cosmologists often employ the method of an effective sound speed[1]. This approach allows one to describe the collective motion of neutrinos in an expanding universe by treating them as a fluid with an effective sound speed. In this thesis, using the method of an effective sound speed in the Einstein-de Sitter model (where the universe is assumed to be matter-dominated) we present a new equation that describes the neutrino density perturbations. We also present approximations to this new equation to simplify the description of the neutrino density perturbations, e.g. the neutrino structure. Additionally, we had originally hoped that we could derive an analytical neutrino bispectrum using the method of an effective sound speed in Einstein-de Sitter. While we were not successful in that regard. We present a small attempt at combing the Newtonian kernel of the matter bispectrum with the neutrino power spectra.

This thesis is structured in the following way

- Chapter 1 serves as an introduction to the basics of cosmology.
- In chapter 2 we present the relevant theoretical background, like the effective sound speed.

- In chapter 3 presents the derivation of the theoretical results. The chapter is structured in such a way as to illustrate our the neutrino equation was derived. we summarize the derivation of the 1st and 2nd order cold dark matter perturbation from [4] and then we derive our neutrino equation.
- In chapter 4 we present our numerical solutions of the differential equations that we worked with, which we then compare with the new equations. In addition, we use the numerical solutions from the code CLASS[5]. We also use the power spectra to test the effectiveness of the numerical solutions of the equations and the neutrino equation.
- In chapter we discuss the results of chapter 4.
- chapter 6 serves as our conclusion.

Chapter 1

The universe

The universe is expanding. This will become relevant.

1.1 The components of the universe

Through analysis of observations, astronomers have come up with a model of the universe with a distribution of the components as depicted in fig. 1.1.

As can be seen on fig. 1.1 there are two types of matter baryonic and dark Matter. Baryonic matter is the matter of the every day, for life on Earth it is what we humans can see with our eyes. Baryonic is a particle physics term that refers to a particle with an odd number of quarks[3].

Although called, dark a more proper term would be non-baryonic matter (do note that there are some theories that suggest that there is baryonic dark matter[7]). Unlike baryonic matter, dark matter does not interact with the electromagnetic spectrum. This means that we can not observe it with light. Explaining what dark matter isn't, does not truly explain what dark matter truly is. The short answer is that we don't really know. Like non-dark matter, dark matter does interact with gravity, meaning that it has mass. We can thus say that dark matter is non-baryonic, non-light-interacting particles with mass. Surprisingly we do know of such a particle, the neutrinos[6].

Neutrinos are an electrically neutral type of particle called leptons (which are spin half particles that do not interact with the strong force but do interact with the weak force[3], another example of leptons would be electrons). They were originally proposed by Pauli so account for the energy and momentum conservation of beta decay. As a result, it has always been a requirement that neutrinos must be very light[3].

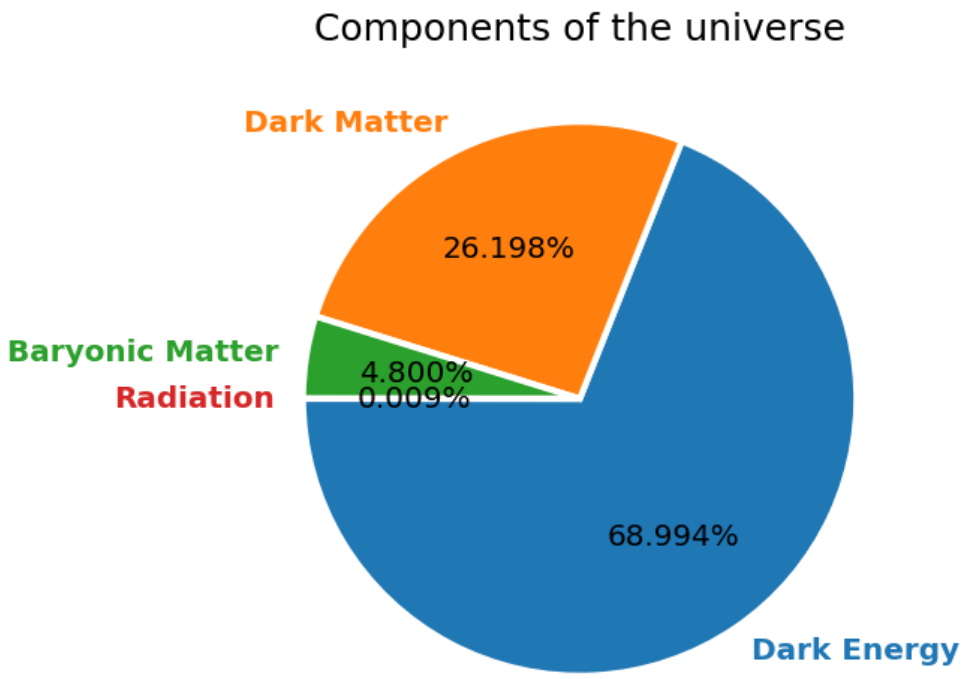

FIGURE 1.1: This figure shows the current partition of stuff in the universe, matter (baryonic and dark), radiation and dark energy. As can be seen, Radiation is effectively zero while "dark" components make up the vast majority of the universe, meanwhile baryonic matter, the matter of our every day makes up less than 5 percent. Based on data from [6] .

However, there is a fundamental problem here and that is the difference between hot and cold. In cosmology, the term hot and cold refers essentially to how relativistic the particles are[6]. If something is hot then it is highly energetic and relativistic, but if it is cold then it means that it is not very energetic and not relativistic and is thus more likely to clump together. While neutrinos are hot, observations generally support the notion that dark matter is cold[6]. Thus dark matter cannot simply be massive neutrinos. In this thesis, we will denote cold dark matter with "CDM".

By structure formation, we mean the clustering togetherness of stuff in the universe. An example of structure would be galaxies. By neutrino structure, we refer to the potential effect on the cosmic structure that neutrinos may have. An in-depth analysis and discussion of the effects of neutrino structure is beyond the scope of this thesis.

1.2 Epochs of the universe

Since which type of particle is dominant in the universe is quite important in this thesis, we will quickly go through the different domination eras of the universe. By domination eras, we refer to the fact that although fig. 1.1 might depict the universe of today it does not show how the universe has always been. Different components have dominated throughout different time periods of the universe. Whichever particle species was dominant at a given time affected how the universe expanded in that time period. The reason for this changing behavior comes about as a consequence of how different particle types are affected differently by the expansion of the universe[6]. Because of this, it is also possible to estimate when which particle species was dominant.

In cosmology, we speak of 4 different eras. The inflation era was a very brief period of time where the universe experienced massive expansion in a very short time, which explains the flatness and uniformity of the universe[6]. Since the inflation era, the universe has had three other eras, where each era has marked the domination of a certain component of the universe. The first era was the radiation domination, lasting from the Big Bang until Radiation-Matter equality at 50000 yrs (at $a = 2.9 \cdot 10^{-4}$[6]), it is the era where subatomic particles and nuclear synthesis took place and the universe was dominated by hot particles ("a" is the scale factor which represents how much smaller the universe was at a given point in time as compared with today). Then came the matter domination era, where the gravitational effects of matter and dark matter became the dominant force in the universe. This era ended when Matter-dark energy equality was reached at 10.2 Gyr (at $a = 0.77$[6]). We are currently in the dark energy era as one can see in fig. 1.1. We don't know much about dark energy and it is currently an active field of study, what we can say is that it is something that is active throughout the universe and is causing the expansion of the universe to accelerate[6].

1.3 Expansion of the universe

In 1929[6] Edwin Hubble discovered that the universe was expanding. This was quite a big deal. What is relevant for us, is how this expansion and its time evolution are explained mathematically and that is through the Hubble parameter, the logarithmic time derivative of a,

$$\frac{\dot{a}}{a} = H, \tag{1.1}$$

The Hubble parameter H has several equations related to it, but for now, the important one is [6]

$$H^2 = H_0^2(\Omega_m/a^3 + \Omega_R/a^4 + \Omega_\Lambda + \frac{1-\Omega_0}{a^2}) \tag{1.2}$$

where H_0 is the Hubble factor, Ω_m is the proportion of matter (baryonic and dark) in the universe today, Ω_R is the proportion of the universe that is radiation and Ω_Λ represents dark energy[6]. The final term represents effects from curvature, with scientists generally agreeing that $\Omega_0 = 1$[8]. This equation tells us how the Hubble parameter and thus the expansion rate and its time evolution are dependent on the components of the universe. As eq. (1.2) is a differential equation one might wish to solve it to get a clear relationship between time and expansion. Unfortunately, there is no simple analytical solution to eq. (1.2)[6]. But if one chooses to focus on a specific time period and thus a specific domination era, we can get away with neglecting the other components in eq. (1.2). As an example and relevant later, if we focus on matter domination, we can let $\Omega_M \to 1$ which reduces eq. (1.2) to

$$H^2 = H_0^2(1/a^3) \tag{1.3}$$

Letting $\Omega_M \to 1$ is a specific type of approximation that we call the Einstein deSitter Universe, which we will use extensively in this thesis.

The Hubble factor is currently one of the most focused-on factors in cosmology as no one can quite agree on its value. The two primary candidates for the value come from [8] with a value of $H_0 = 67.27 \pm 0.6 \text{kms}^{-1}\text{Mpc}^{-1}$ and from [9] with a value of $H_0 = 73.2 \pm 1.3 \text{kms}^{-1}\text{Mpc}^{-1}$. We choose to work with $H_0 = 68$ km/s/Mpc .

As stated the scale factor represents how much the universe has expanded between two time periods, where we set the scale of today to 1[6]. One way of calculating a is as a function of redshift

$$a = \frac{1}{z+1} \tag{1.4}$$

where z is the redshift.

Chapter 2

Theory

2.1 On Notation

To avoid confusion we start off by summarizing the notation used. In some parts of this thesis, the "Einstein summation" notation was used, where indices that repeat, represent an implicit summation. As an example $x_\mu x^\mu$ represents

$$x_\mu x^\mu = \sum_{\mu=0}^{3} x_\mu x^\mu = x_0 x^0 + x_1 x^1 + x_2 x^2 + x_3 x^3 \tag{2.1}$$

when Greek letters are used, we summarized the time and spacial components while Latin indices only represent spacial components, so

$$x_\mu x^\mu = x_0 x^0 + x_i x^i. \tag{2.2}$$

We will also use two forms of shorthand for differentiation, the first is

$$\partial_i = \frac{\partial}{\partial^i} \tag{2.3}$$

and the second is

$$A_{,\alpha} = \frac{\partial A}{\partial x^\alpha}. \tag{2.4}$$

Unless specifically stated we will use natural units

$$\hbar = c = k_B = 1. \tag{2.5}$$

We also need to discuss our time variables, in cosmology it is common practice to use different types of time variables. There is the standard physical time

that is used in most of physics, then there is conformal time (τ) where we take into account the expansion of the universe using the transformation

$$dt = ad\tau. \tag{2.6}$$

Having explained the difference in physical and conformal time it is relevant to bring up their different representations of the Hubble parameter,

$$\mathcal{H} = \frac{1}{a}\frac{\mathrm{d}a}{\mathrm{d}\tau}, \quad H = \frac{1}{a}\frac{\mathrm{d}a}{\mathrm{d}t}. \tag{2.7}$$

This means that the conformal Hubble parameter is also equal to

$$\begin{aligned}\mathcal{H} &= \frac{1}{a}\frac{\mathrm{d}a}{\mathrm{d}\tau} = \frac{1}{a}\frac{\mathrm{d}a}{\mathrm{d}\tau}\frac{\mathrm{d}t}{\mathrm{d}t} = \frac{1}{a}\frac{\mathrm{d}t}{\mathrm{d}\tau}\frac{\mathrm{d}a}{\mathrm{d}t} = \frac{\mathrm{d}a}{\mathrm{d}t} = aH \\ &= H_0^2\sqrt{\Omega_M/a + \Omega_r/a^2 + \Omega_\Lambda a^2 + (1-\Omega_0)}\end{aligned} \tag{2.8}$$

Finally, we may also use the scale factor as a time variable.

2.2 General relativity

The main difference between classical Newtonian physics and general relativity (GR) is that in GR time and space are not separate and our coordinate systems may begin to experience curvature. Like with special relativity, there is also a huge emphasis on how things are observed in different reference frames. An important part of GR is the metric $g_{\mu\nu}$, which is used to describe the curvature of a given system. There is also a big focus on invariant terms, chief among these being the space-time interval squared[10]

$$ds^2 = g_{\mu\nu}dx^\mu dx^\nu \tag{2.9}$$

with $dx = (dt, dx, dy, dz)$ representing infinitesimal changes in space time. The behavior/curvature of a given system may then be described using the metric, as an example in flat Euclidean space $g_{\mu\nu} = diag(-1, 1, 1, 1)$, called the Minkowski metric[10]

$$ds^2 = -dt^2 + dx^2 + dy^2 + dz^2 = -dt^2 + dr^2 \tag{2.10}$$

where we collect the spacial coordinates into dr.
Another difference between GR and Newton is the equation of motion for a free object. In Newtonian mechanics,

$$\frac{d^2x^i}{dt^2} = 0 \tag{2.11}$$

where x is position, in GR the motion of a free object is described by the geodesic equation[10]

$$\frac{d^2x^\mu}{d\lambda^2} + \Gamma^\mu_{\alpha\beta}\frac{dx^\alpha}{d\lambda}\frac{dx^\beta}{d\lambda} = 0 \tag{2.12}$$

where the gammas are Christoffel symbols that describe the curvature of space [10]

$$\Gamma^\alpha_{\mu\nu} = \frac{1}{2}g^{\alpha\beta}(g_{\nu\beta,\mu} + g_{\beta\mu,\nu} - g_{\mu\nu,\beta}). \tag{2.13}$$

We then move on to the governing equation of GR, the Einstein equation[10]

$$G_{\mu\nu} = R_{\mu\nu} - \frac{1}{2}\mathcal{R}g_{\mu\nu} = 8\pi G T_{\mu\nu}, \tag{2.14}$$

where G is the gravitational constant, $T_{\mu\nu}$ is the energy-momentum tensor and $R_{\mu\nu}$ and $\mathcal{R}$ are the Ricci tensor and Ricci scalar ($\mathcal{R} = g^{\mu\nu}R_{\mu\nu}$) respectively. The Ricci tensor is given in terms of Christoffel symbols [10]

$$R_{\alpha\nu} = \partial_\mu\Gamma^\mu_{\nu\alpha} - \partial_\nu\Gamma^\mu_{\mu\alpha} + \Gamma^\mu_{\nu\lambda}\Gamma^\lambda_{\mu\alpha} - \Gamma^\mu_{\nu\lambda}\Gamma^\lambda_{\mu\alpha}, \tag{2.15}$$

and is meant to give a measure of the general curvature of a given space. The energy-momentum tensor and as its name suggest describes the energy and momentum of a system and so the point of the Einstein equation is to describe the relationship between the curvature of space and its energy and momentum.

2.3 The Friedmann equations

eq. (2.14) is essentially a long list of differential equations which we can use to describe the curvature and behavior of space. Simplifications and generalizations are thus to be expected. If we assume that the universe is filled up with an isotropic, perfect and homogeneous fluid, then the metric needed to describe the universe can be written as

$$ds^2 = -dt^2 + a(t)^2\left[dr^2 + S_k(r)^2 d\Omega^2\right] \tag{2.16}$$

where $d\Omega^2$ represent spherical coordinates[6] and S_k is a curvature dependent function given as

$$S_k = \begin{cases} R_0\sin(r/R_0) & (\kappa = +1) \\ r & (\kappa = 0) \\ R_0\sinh(r/R_0) & (\kappa = -1) \end{cases}, \tag{2.17}$$

where κ represents the curvature and R_0 is the radius of curvature[6]. eq. (2.16) is called the Friedmann-Lemaître-Robertson-Walker metric[6] and from it, we can derived[6]

$$H^2 = \frac{8\pi G}{3}\varepsilon(t) - \frac{\kappa}{R_0^2 a(t)^2}, \tag{2.18}$$

where ε is the energy density[6]. As the universe is generally accepted to be flat[8] we set $\kappa = 0$, additional equations can then be derived from the Friedmann metric to describe the universe, one important equation is[6]

$$\frac{\ddot{a}}{a} = -\frac{4\pi G}{3}(\rho + 3P) \tag{2.19}$$

where P is the pressure and ρ the energy density of the components of the universe (eq. (2.18) and eq. (2.19) are called the Friedmann equations[6]). This equation tells us that the behavior of expansion comes down to a relation between the energy and pressure of the components of the universe. Here it is useful to use the equation of state parameter $w = P/\rho$[2]. w varies for different components of the universe. For radiation $w = 1/3$ for matter $w = 0$ and for dark energy $w = -1$[6].

2.4 Particles in cosmology

As we are interested in the structure formation of different particle species, we wish to understand how their density and velocity evolve. To derive equations that describe that, we turn to the Boltzmann equation, as it provides a framework for describing the statistical behavior of and interactions between particles[2]

$$\frac{\mathrm{d}f}{\mathrm{d}t} = \frac{\partial f}{\partial t} + \frac{\partial f}{\partial x^i}\frac{\mathrm{d}x^i}{\mathrm{d}t} + \frac{\partial f}{\partial p}\frac{\mathrm{d}p}{\mathrm{d}t} + \frac{\partial f}{\partial \hat{p}^i}\frac{\mathrm{d}\hat{p}^i}{\mathrm{d}t} = C[f] \tag{2.20}$$

where f is the distribution function in phase space (a space where both position and momentum are coordinates $(\boldsymbol{x}, \boldsymbol{p})$), C represents all possible collision terms, x represents position, p momentum and $\hat{p}^i$ is the momentum unit vector.

2.4.1 Cold dark matter

As an important example, we have dark matter. When working with eq. (2.20) a problem that often comes up is that the collision term adds a great deal of complicity, see for example [2]. Because dark matter does not interact with other particles there are no collision terms and thus the right-hand side of eq. (2.20) is zero. Now we will refer to [4] for a step-by-step guide, but briefly said, using that the collision term must be zero and standard cosmology assumptions, we get that the behavior of the density contrast δ and the divergence of the velocity flow θ are govern by[4],

$$\dot{\delta} = -\partial_j\left[(1+\delta)\partial_j\nabla^{-2}\theta\right] \tag{2.21}$$

$$\dot{\theta} = \mathcal{H}\theta - \partial_i\partial_j\nabla^{-2}\theta\partial_j\partial_i\nabla^{-2}\theta - \partial_j\nabla^{-2}\theta\partial_j\theta - \frac{3}{2}\frac{H_0^2\Omega_m}{a}\delta, \tag{2.22}$$

where ∇^{-2} is the inverse Laplace operator.

2.4.2 Massive neutrinos

What separates the description of neutrinos from that of dark matter, is that for the neutrinos a hierarchy of equations is needed. We start with our distribution function which we write as

$$f(x, \boldsymbol{p}, \tau) = f_0(p)\big[1 + \Psi(x, \boldsymbol{p}, \tau)\big] \tag{2.23}$$

where $f_0(p)$ is the zeroth-order phases space distribution and Ψ is the perturbation component[11]. Quantities like energy density and pressure of a particle are derived via momentum integrals, examples would be the pressure and the pressure perturbation[11]

$$P = \frac{1}{3}a^{-4}\int q^2 dq d\Omega \frac{q^2}{\epsilon} f_0(q) \quad \delta P = \frac{1}{3}a^{-4}\int q^2 dq d\Omega \frac{q^2}{\epsilon} f_0(q)\Psi \tag{2.24}$$

where q is the comoving momentum ($q \equiv ap$) and Ω represents spherical integration.
However, for massive neutrinos, we cannot simply integrate out the momentum given the dependence on the momentum by the energy ϵ[11]. So we expand the perturbation in a Legendre series[11]

$$\Psi(\boldsymbol{k}, p, \tau) = \sum_{l=0}^{\infty}(-i)^l(2l+1)\Psi_l(\boldsymbol{k}, p, \tau)P_l(\hat{k}\cdot\hat{n}), \tag{2.25}$$

where P_l is the Legendre polynomials and $\boldsymbol{k}$ is the scale. This means that the equations for the perturbed density, pressure, energy flow and shear stress (respectively) are now

$$\delta\rho = 4\pi a^{-4}\int q^2 dq \epsilon f_0(q)\Psi_0 \tag{2.26}$$

$$\delta P = \frac{4\pi}{3}a^{-4}\int q^2 dq \frac{q^2}{\epsilon} f_0(q)\Psi_0 \tag{2.27}$$

$$(\bar{\rho}_h + \bar{P}_h)\theta_h = 4\pi k a^{-4}\int q^2 dq q f_0(q)\Psi_1 \tag{2.28}$$

$$(\bar{\rho}_h + \bar{P}_h)\sigma_h = \frac{8\pi}{3}a^{-4}\int q^2 dq \frac{q^2}{\epsilon} f_0(q)\Psi_2 \tag{2.29}$$

where the bar denotes the unperturbed components. The challenge is that these perturbation components are coupled to each other, as such

$$\dot{\Psi}_0 = -\frac{qk}{\epsilon}\Psi_1 - \dot{\phi}\frac{\mathrm{d}\ln f_0}{\mathrm{d}\ln q} \tag{2.30}$$

$$\dot{\Psi}_1 = -\frac{qk}{\epsilon}(\Psi_0 - 2\Psi_2) - \frac{\epsilon k}{3q}\psi\frac{\mathrm{d}\ln f_0}{\mathrm{d}\ln q} \tag{2.31}$$

$$\dot{\Psi}_l = \frac{qk}{(2l+1)\epsilon}[l\Psi_{l-1} - (l+1)\Psi_{l+1}], \quad l \geq 2 \tag{2.32}$$

(these equations are in the conformal Newtonian gauge). Because this hierarchy of equations is infinite, the standard approach[11] is to truncate at some $\Psi_{l_{max}}$.

2.4.3 A neutrino sound speed

In the previous section, we spook about truncating the neutrino hierarchy of equations at some l_{max}. One approach is to use the adiabatic approximation which means that we set the shear stress term σ to zero, meaning that $\Psi_2 = 0$. Instead of looking at the integral version of θ and δ (note that $\delta = \delta\rho/\bar{\rho}$) we look at the differential versions [11]

$$\dot{\delta} = -(1+w)(\theta - 3\dot{\phi}) - 3\frac{\dot{a}}{a}\Big(\frac{\delta P}{\delta\rho} - w\Big)\delta \tag{2.33}$$

$$\dot{\theta} = -\frac{\dot{a}}{a}(1-3w)\theta - \frac{\dot{w}}{1+w}\theta + \frac{\delta P/\delta\rho}{1+w}k^2\delta - k^2\sigma + k^2\psi \tag{2.34}$$

where ϕ is the perturbation on the metric, w is the equation of state and $k^2\psi$ represents gravity[12, 4].
Now these are the generalized versions of δ and θ. In our case of working in the Newtonian limit deep in matter domination with the adiabatic approximation eq. (2.33) and eq. (2.34) reduce to

$$\dot{\delta} = -\theta \tag{2.35}$$

$$\dot{\theta} = -\frac{\dot{a}}{a}\theta + \frac{\delta P}{\delta\rho}k^2\delta + k^2\psi. \tag{2.36}$$

The standard approach in the literature [1] is then to introduce the effective sound speed

$$c_s^2 = \frac{\delta P}{\delta\rho}. \tag{2.37}$$

Now the actual value for this sound speed is[1, 11]

$$c_s^2 \equiv \frac{\delta P}{\delta\rho} = \frac{1}{3}\frac{\int q^2 dq \frac{q^2}{\varepsilon(q)} f_0(q)\Psi_0}{\int q^2 dq \varepsilon(q) f_0(q)\Psi_0} \tag{2.38}$$

Instead of solving this equation, it is common in the literature to set the sound speed equal to the velocity dispersion[1]

$$c_s^2 \equiv \sigma_v^2 = \langle v^2\rangle - \langle v\rangle^2. \tag{2.39}$$

Since $\langle v\rangle = 0$ we then have

$$c_s^2 = \sigma_v^2 = \frac{\int q^2 dq (\frac{q}{m_\nu})^2 f_0(q)}{\int q^2 dq f_0(q)} = \frac{T_{\nu,0}^2}{m_\nu^2}\frac{\int dx \frac{x^4}{e^x+1}}{\int dx \frac{x^2}{e^x+1}} = 15\frac{\zeta(5)}{\zeta(3)}\frac{T_\nu^2}{m_\nu^2}. \tag{2.40}$$

where T_ν is the temperature of the neutrinos. That was all done assuming that the shear stress σ and thus Ψ_2 are zero. However, it is worth pointing

out that something is lost by simply setting $\sigma = 0$ and stating that eq. (2.38) can simply be replaced by eq. (2.40) [1]. We will thus follow [1] where we compensate for this by setting

$$c_s^2 = \frac{5}{9}\sigma_v^2 = \frac{25}{3}\frac{\zeta(5)}{\zeta(3)}\frac{T_\nu^2}{m_\nu^2} = \frac{25}{3}\frac{\zeta(5)}{\zeta(3)}\frac{T_{\nu,0}^2(1+z)^2}{m_\nu^2} \tag{2.41}$$

where we have rewritten temperature as the current neutrino temperature and $(1+z)^2$. With that, we may then state that our approximate equation for the neutrino in the Newtonian limit using the effective sound speed of neutrinos gives us

$$\dot{\delta}_\nu = -\theta_\nu \tag{2.42}$$

$$\dot{\theta} = -\frac{\dot{a}}{a}\theta + c_s(a)^2 k^2 \delta + k^2 \psi. \tag{2.43}$$

2.5 Correlation Functions

The universe is homogeneous on very large scales, but not on smaller scales. There are inhomogeneities on smaller scales. We describe these with the density contrast δ

$$\rho(\boldsymbol{x}) = (1 + \delta(\boldsymbol{x}))\bar{\rho} \tag{2.44}$$

where $\bar{\rho}$ is the mean density in the universe and $\rho(x)$ is the density at position $\boldsymbol{x}$. As mentioned, it is quite important to consider which scale we are considering. An easy way to distinguish between scales is to Fourier transform $\delta(\boldsymbol{x})$ which then becomes $\delta(\boldsymbol{k})$, where k corresponds to different scales. The relation is inverse, so the smaller k is the large the scale we are dealing with is. Now because of the definition of $\delta(\boldsymbol{x})$ taking an average (doing a volume integral) would yield $\langle\delta(x)\rangle = 0$. But that is not the case if you look at correlation functions,

$$\xi_2 = \langle\delta(x_1)\delta(x_2)\rangle \tag{2.45}$$

$$\xi_3 = \langle\delta(x_1)\delta(x_2)\delta(x_3)\rangle \tag{2.46}$$

$$\xi_N = \langle\delta(x_1)\delta(x_2)...\delta(x_N)\rangle \tag{2.47}$$

The correlation functions are defined as the joint density average at N different locations[13]. In other words, what is the expectation value of the product of n perturbations in different positions[14]. As mentioned it can be useful to work in Fourier space, this turns the two-point correlation function into

$$\langle\tilde{\delta}(\boldsymbol{k})\tilde{\delta}(\boldsymbol{k}')\rangle = \int d^3x d^3x' \xi_2(x') e^{-i(k+k')x - ik'x'} \tag{2.48}$$

$$(2\pi)^3\delta^3(k+k')\int d^3x' \xi_2(x') e^{ikx'} = (2\pi)^3\delta^3(\boldsymbol{k}+\boldsymbol{k}')P(k) \tag{2.49}$$

where $\delta^3()$ is the Dirac delta function and $P(k)$ is the power spectrum[13]. To numerically calculate the power spectrum we used [15]

$$P(k) = 2\pi^2 Y^2(\tau, k) k^{-3} \mathcal{P}(k) \tag{2.50}$$

where Y is the quantity that we make the power spectrum of (in our case δ for CDM and neutrinos) and $\mathcal{P}(k)$ is the primordial power spectrum.

Now we have seen how one can express the Fourier transformations of the two-point correlation function, but this is not restricted to 2 points and is possible for all correlation functions as [13]

$$\langle \delta(\boldsymbol{k_1}) .. \delta(\boldsymbol{k_N}) \rangle = (2\pi)^3 \delta^3(\boldsymbol{k_1} + ... + \boldsymbol{k_N}) P_N(\boldsymbol{k_1}, ..., \boldsymbol{k_N}). \tag{2.51}$$

The Bispectrum is the name of the 3-point correlation function, which is then an indicator of the variance between 3 points. For calculating the bispectrum we use [4]

$$B(k_1, k_2, k_3) = 2\{P(k_1)P(k_2)\boldsymbol{\mathcal{K}}(k_1, k_2, k_3) + 2\text{Perm}\} \tag{2.52}$$

where $\boldsymbol{\mathcal{K}}$ is a kernel. The $\boldsymbol{\mathcal{K}}$ for total matter is derived in section 3.2.

Chapter 3

Analytical Results

The structure of this chapter is as follows. First, we derived the first-order cold dark matter perturbation, then the second order perturbation in ΛCDM. Then we showed the effects of switching to Einstein-de Sitter. Then we will do it for neutrinos and we show what we manage to accomplish there.

As a reminder perturbation theory is a method of approximating equations by "expanding" the functions to a certain order, like

$$\delta = \delta^{(1)} + \frac{1}{2}\delta^{(2)} \tag{3.1}$$

Then we insert these expansions into the equations and ignore everything that is above our order of expansion (for the case of a 2nd order expansion, a term like $\delta^{(1)}\delta^{(2)}$ which is a 3rd order term and would be neglected).

To begin, we note that we closely follow the derivation for first and second order cold dark matter perturbation in [4]. We repeat it here for clarity.

3.1 First order cold dark matter

We start off by taking the first order expansion of δ and θ in eq. (2.21) and eq. (2.22), this gives us (in conformal time)

$$\dot{\delta}^{(1)} = -\theta^{(1)} \tag{3.2}$$

$$\dot{\theta}^{(1)} = -\mathcal{H}\theta^{(1)} - \frac{3}{2}\frac{H_0^2\Omega_M}{a}\delta^{(1)}, \tag{3.3}$$

combining these equations of motion we get

$$\ddot{\delta}^{(1)} + \mathcal{H}\dot{\delta}^{(1)} = \frac{3}{2}\frac{H_0^2\Omega_M}{a}\delta^{(1)}. \tag{3.4}$$

δ and θ are time and space dependent, but as there are no explicit space dependent terms in eq. (3.4) we split the dependencies up as $\delta^{(1)}(\tau, x) = D(\tau)\tilde{\delta}(x)$, we can then insert this into eq. (3.4) and we gain a purely time-dependent equation,

$$\ddot{D} + \mathcal{H}\dot{D} - \frac{3}{2}\frac{H_0^2\Omega_M}{a}D = 0. \tag{3.5}$$

So we see that we have a differential equation for the time component of $\delta^{(1)}$. As for $\theta^{(1)}$ we can reexpress it as $\theta^{(1)} = -\frac{\dot{D}}{D}\delta^{(1)}$. We then go to the second order.

3.2 Second order cold dark matter

To find the second order equation for dark Matter, we start off by taking the second order expansion of δ and θ

$$\delta = \delta^{(1)} + \frac{1}{2}\delta^{(2)}$$
$$\theta = \theta^{(1)} + \frac{1}{2}\theta^{(2)}.$$

combining these expansions with eq. (2.21), eq. (2.22), eq. (3.2) and eq. (3.3) we get two 2nd order equations

$$\dot{\delta}^{(2)} = -2\partial_j\nabla^{-2}\theta^{(1)}\partial_j\delta^{(1)} - 2\delta^{(1)}\theta^{(1)} - \theta^{(2)} \tag{3.6}$$

$$\dot{\theta}^{(2)} = -\mathcal{H}\theta^{(2)} - 2\Big(\partial_j\partial_i\nabla^{-2}\theta^{(1)}\partial_i\partial_j\nabla^{-2}\theta^{(1)}\Big) - 2\partial_j\nabla^{-2}\theta^{(1)}\partial_j\theta - \frac{3}{2}\frac{H_0^2\Omega_M}{a}\delta^{(2)}. \tag{3.7}$$

We then combine eq. (3.6) and eq. (3.7) into a single second order differential equation,

$$\begin{aligned}\ddot{\delta}^{(2)} + \mathcal{H}\dot{\delta}^{(2)} =& 2\Big(\mathcal{H}\dot{D}D + \ddot{D}D + \dot{D}^2\Big)\Big[\partial_j\nabla^{-2}\tilde{\delta}\partial_j\tilde{\delta} + \tilde{\delta}^2\Big] + \frac{3}{2}\frac{H_0^2\Omega_m}{a}\delta^{(2)} \\ &+ 2\dot{D}^2\Big[\partial_i\partial_j\nabla^{-2}\tilde{\delta}\partial_i\partial_j\nabla^{-2}\tilde{\delta} + \partial_j\nabla^{-2}\tilde{\delta}\partial_j\tilde{\delta}\Big].\end{aligned} \tag{3.8}$$

The solution to eq. (3.8) is given as [4]

$$\begin{aligned}\delta^{(2)} =& 2\partial_j\nabla^{-2}\delta^{(1)}\partial_j\delta^{(1)} + \Big(1 + \frac{F}{D^2}\Big)\delta^{(1)}\delta^{(1)} \\ &+ \Big(1 - \frac{F}{D^2}\Big)\partial_i\partial_j\nabla^{-2}\delta^{(1)}\partial_i\partial_j\nabla^{-2}\delta^{(1)}\end{aligned} \tag{3.9}$$

Where F is a function which is governed by

$$\ddot{F} + \mathcal{H}\dot{F} = \frac{3}{2}\frac{H_0^2\Omega_M}{a}\Big(F + D^2\Big). \tag{3.10}$$

Although it is a solution eq. (3.9) is still rather complex. To simplify we switch to Fourier space, which turns eq. (3.9) into

$$\frac{1}{2}\delta^{(2)}(k) = C_k\left\{\mathcal{K}_N(k_1,k_2,k)\delta^{(1)}(k_1)\delta^{(1)}(k_2)\right\}, \tag{3.11}$$

with

$$\mathcal{K}_N(k_1,k_2,k) \equiv (\beta_N - \alpha_N) + \frac{\beta_N}{2}\hat{\boldsymbol{k}}_1\cdot\hat{\boldsymbol{k}}_2\left(\frac{k_2}{k_1}+\frac{k_1}{k_2}\right) + \alpha_N\left(\hat{\boldsymbol{k}}_1\cdot\hat{\boldsymbol{k}}_2\right)^2 \tag{3.12}$$

and

$$\alpha_N = \frac{7-3v}{14}, \quad \beta_N = 1, \quad v = 7F/3D^2, \tag{3.13}$$

where C_k is the convolution integral,

$$C_k\{f(\boldsymbol{k}_1,\boldsymbol{k}_2)\} \equiv \int \frac{d\boldsymbol{k}_1\boldsymbol{k}_2}{(2\pi)^3} f(\boldsymbol{k}_1,\boldsymbol{k}_2)\delta^D(\boldsymbol{k}-\boldsymbol{k}_1-\boldsymbol{k}_2) \tag{3.14}$$

We now have the equation for the second order equation in Λ_{cdm} and a Kernel which we could use to generate a CDM bispectrum (as mentioned in section 2.5). With this summary of the Newtonian section of [4] we now switch to Einstein-de Sitter Universe.

3.3 Dark Matter using the Einstein-de Sitter Model

We will go in the reversed order here and briefly talk about the second order first. This comes from the fact that for second order CDM, the only difference between the Λ_{cdm} and Eisntein-de Sitter is that the kernel eq. (3.11) is altered so that in eq. (3.13) $v \to 1$ and thus $\alpha_N \to 2/7$[4]. This marks the end of the [4] walkthrough and we turn to the first order.

As discussed previously, the main principle of Einstein-de Sitter is the assumption that there is only matter in the universe, e.g. $\Omega_M \simeq 1$. This has the effect of reducing the Hubble parameter to (in conformal time)

$$\mathcal{H} = \frac{\dot{a}}{a} = H_0\sqrt{\Omega_M/a} = \frac{H_0}{\sqrt{a}}, \tag{3.15}$$

which lets us analytically solve for the scale factor

$$\dot{a} = H_0\sqrt{a} \to a = \frac{1}{4}H_0^2\tau^2, \tag{3.16}$$

This means that we can rewrite eq. (3.5) as

$$\ddot{D} + \mathcal{H}\dot{D} - \frac{3}{2}\frac{H_0^2\Omega_M}{a}D = 0.$$

as

$$\ddot{D} + \frac{H_0}{\sqrt{a}}\dot{D} = \frac{3}{2}\frac{H_0^2}{a}D. \tag{3.17}$$

$$\ddot{D} + 2\frac{H_0}{H_0\tau}\dot{D} = 4\frac{3}{2}\frac{H_0^2}{H_0^2\tau^2}D. \tag{3.18}$$

$$\ddot{D} + \frac{2}{\tau}\dot{D} = \frac{6}{\tau^2}D. \tag{3.19}$$

This is a solvable equation but instead of solving it in conformal time, we choose to switch to scale time.Equation (3.19) rewritten in scaletime becomes[1]

$$a^2\ddot{D} + \frac{3}{2}a\dot{D} = \frac{3}{2}D \tag{3.20}$$

Equation (3.20) has the simple solution of

$$D \propto a \tag{3.21}$$

$$D = D_0 a, \tag{3.22}$$

where D_0 is a factor dependent on initial conditions. We will come back to eq. (3.22) but for now we move unto the neutrinos.

3.4 First order neutrinos

We will be working in Fourier space in this section. So when we write δ_ν and θ_ν we mean the Fourier transform of δ_ν and θ_ν. We used eq. (2.42) and eq. (2.43). One important note is that the neutrino equations for δ_ν and θ_ν will not experience gravity from the neutrinos. This is because we make the assumption, like in [1], that the neutrino sourcing may be neglected as it is minute compared with the CDM sourcing. We replace the gravity term in eq. (2.43) with $\frac{3}{2}\frac{H_0^2\Omega_M}{a}\delta_{\text{cdm}}$[4] giving us[2]

$$\dot{\delta}_\nu^{(1)} = -\theta_\nu^{(1)} \tag{3.23}$$

$$\dot{\theta}_\nu^{(1)} = -\mathcal{H}\theta_\nu^{(1)} - \frac{3}{2}\frac{H_0^2\Omega_M}{a}\delta_{cdm}^{(1)} + k^2 c_s(a)^2\delta_\nu^{(1)} \tag{3.24}$$

$$\ddot{\delta}_\nu^{(1)} + \mathcal{H}\dot{\delta}_\nu^{(1)} = \frac{3}{2}\frac{H_0^2\Omega_M}{a}\delta_{\text{cdm}}^{(1)} - k^2 c_s(a)^2\delta_\nu^{(1)}. \tag{3.25}$$

1: See appendix for derivation.

2: See Appendix for derivation of eq. (3.25)

With that done we then switch from conformal time to scale time [3]

$$\left(\frac{3}{2}\Omega_M + 3\Omega_\Lambda a^3\right)\dot{\delta}_\nu^{(1)} + \left(a\Omega_m + a^4\Omega_\Lambda\right)\ddot{\delta}_\nu^{(1)} = \frac{3}{2}\frac{\Omega_m}{a}\delta_{\text{cdm}}^{(1)} - \frac{k^2 c_s(a)^2}{H_0^2}\delta_\nu^{(1)}. \quad (3.26)$$

To simplify we then switch to the Einstein-de Sitter Model

$$\frac{3}{2}\dot{\delta}_\nu^{(1)} + a\ddot{\delta}_\nu^{(1)} = \frac{3}{2}\frac{1}{a}\delta_{\text{cdm}}^{(1)} - \frac{k^2 c_s(a)^2}{H_0^2}\delta_\nu^{(1)}. \quad (3.27)$$

Besides simplifying eq. (3.26) the reason why we use the Einstein-de Sitter is so that we may use the solution to the $\delta_{\text{cdm}}^{(1)}$ from eq. (3.22). Using that we may rewrite eq. (3.27) as

$$\frac{3}{2}\dot{\delta}_\nu^{(1)} + a\ddot{\delta}_\nu^{(1)} = \frac{3}{2}\frac{1}{a}aD_0 - \frac{k^2 c_s(a)^2}{H_0^2}\delta_\nu^{(1)}. \quad (3.28)$$

$$\frac{3}{2}\dot{\delta}_\nu^{(1)} + a\ddot{\delta}_\nu^{(1)} = \frac{3}{2}D_0 - \frac{k^2 c_s(a)^2}{H_0^2}\delta_\nu^{(1)}. \quad (3.29)$$

Which we rearrange

$$\frac{3}{2}\dot{\delta}_\nu^{(1)} + a\ddot{\delta}_\nu^{(1)} + \frac{k^2 c_s(a)^2}{H_0^2}\delta_\nu^{(1)} = \frac{3}{2}D_0. \quad (3.30)$$

This differential equation has a solution[4]

$$\delta_\nu^{(1)} = aD_0 + c_1\cos\left(\frac{2kc_s(a)\sqrt{a}}{H_0}\right) - c_2\sin\left(\frac{2kc_s(a)\sqrt{a}}{H_0}\right) \quad (3.31)$$

$$+ \left(\frac{2kc_s(a)a}{H_0}\right)^2 D_0\Bigg[\cos\left(\frac{2kc_s(a)\sqrt{a}}{H_0}\right)\text{Ci}\left(\frac{2kc_s(a)\sqrt{a}}{H_0}\right) \quad (3.32)$$

$$+ \sin\left(\frac{kc_s(a)\sqrt{a}}{H_0}\right)\text{Si}\left(\frac{kc_s(a)\sqrt{a}}{H_0}\right)\Bigg], \quad (3.33)$$

where Ci and Si are the cosine and sine integrals respectively. To make this equation a bit more readable we introduce the variable

$$M(a) = \left(\frac{2kc_s(a)\sqrt{a}}{H_0}\right)$$

$$\delta_\nu^{(1)} = aD_0 + c_1\cos(M(a)) - c_2\sin(M(a)) \quad (3.34)$$

$$+ aM(a)^2 D_0\left[\cos(M(a))\text{Ci}(M(a)) + \sin(M(a))\text{Si}(M(a))\right] \quad (3.35)$$

3: see appendix

4: Solved using Mathematica

We need to specify the factors c_1 and c_2. It was not possible for us to use Mathematica to find c_1 and c_2 when using initial conditions so we found another way. To do this let us think a bit about the equation. This equation is meant to represent the δ_ν in a matter-dominated universe. This means that it will start out oscillating until a certain point, where the effects of gravity will start to dominate the neutrinos and so they will start to follow the CDM. we can thus interpret terms with D_0 as representations of the dark matter and the interplay between the effects of gravity and the neutrino sound speed. The terms with c_1 and c_2 are the cos and sin terms, e.g. the oscillating terms, representing the oscillating behavior of the neutrinos before they start to experience the effect of the CDM. This is then our justification for doing an expansion around $a = 0$ as we will retain the coefficients but the equation will reduce in complexity.
So we expanded around $a = 0$ giving

$$\delta_\nu = c_1 \cos\Big(M(a)\Big) - (2\pi P - c_2)\sin\Big(M(a)\Big), \tag{3.36}$$

with us defining $P \equiv D_0\left(\frac{kc_s(a)a}{H_0}\right)^2$. It is worth noting that because the sound speed is proportional to $1/a$, P is actually a constant. We then claim that we can rewrite eq. (3.36) as simply a cosine,

$$\delta_\nu = A\cos(M(a) + \Phi) \tag{3.37}$$

with Φ being phase. Using trigonometry we can rewrite eq. (3.37) as

$$\delta_\nu = A\cos(M(a))\cos(\Phi) + \sin(M(a))\sin(\Phi) \tag{3.38}$$

if we now set $\Phi = 0$ then eq. (3.37) and eq. (3.38) will be equivalent to eq. (3.36) if

$$c_1 = A \; c_2 = 2\pi P \tag{3.39}$$

With that we have a value of c_2 but what about c_1 what is A? Another reason that we rewrote the expansion as eq. (3.37) is that we can then do the following. Taking the derivative of δ_ν we get

$$\dot{\delta}_\nu = -A\dot{M}(a)\sin(M(a)) \tag{3.40}$$

which means that

$$\delta_\nu^2 + (\dot{\delta}_\nu/\dot{M}(a))^2 = A^2(\cos^2(M(a)) + \sin^2(M(a))) = A^2 \tag{3.41}$$

meaning that

$$A = \sqrt{\delta_\nu^2 + (\dot{\delta}_\nu/\dot{M}(a))^2}. \tag{3.42}$$

With that, all we need is some initial value of $\delta_\nu^{(1)}$ and $\dot{\delta}_\nu^{(1)}$ at some value of a, $a_{initial}$ (which we denote a_0) and we have an equation for the neutrino density perturbation in a matter-dominated universe

$$M(a) = \left(\frac{2kc_s(a)\sqrt{a}}{H_0}\right) = 5\sqrt{\frac{\zeta 5}{3\zeta 3}}\left(\frac{2kT_{\nu,0}}{m_\nu H_0\sqrt{a}}\right) \tag{3.43}$$

$$A = \sqrt{\delta(a_0)_\nu^2 + (\dot{\delta}(a_0)_\nu/\dot{M}(a_0))^2} \quad P \equiv D_0\left(\frac{kc_s(a)a}{H_0}\right)^2$$

$$\begin{aligned}\delta_\nu^{(1)} =& aD_0 + A\cos\Big(M(a)\Big) - 2\pi P\sin\Big(M(a)\Big) \\ &+ aM(a)^2 D_0\Big[\cos\Big(M(a)\Big)\mathrm{Ci}(M(a)) + D_0\sin(M(a))\mathrm{Si}(M(a))\Big]\end{aligned} \tag{3.44}$$

This is the main result of this thesis.

3.5 2nd order neutrinos

We also tried to derive a second order equation for the neutrinos although we did not succeed. Our logic was that since eq. (3.25) was so similar to eq. (3.4), it might be the case that something similar is the case for the second order equations. Therefore we took the equations of eq. (2.21) and eq. (2.22) and inserted an effective sound speed

$$\dot{\delta}_\nu = -\partial_j\Big[(1+\delta_\nu)\partial_j\nabla^{-2}\theta_\nu\Big] \tag{3.45}$$

$$\dot{\theta}_\nu = \mathcal{H}\theta_\nu - \partial_i\partial_j\nabla^{-2}\theta_\nu\partial_j\partial_i\nabla^{-2}\theta_\nu - \partial_j\nabla^{-2}\theta_\nu\partial_j\theta_\nu - \frac{3}{2}\frac{H_0^2\Omega_m}{a}\delta_{\mathrm{cdm}} + c_s^2\nabla^2\delta_\nu. \tag{3.46}$$

where write the effective sound speed term as $c_s^2\nabla^2\delta_\nu$ like in [16].

Then taking our equations for the first order terms and taking the second order of eq. (3.45) and eq. (3.46) we get[5]

$$\dot{\delta}_\nu^{(1)} = -\theta_\nu^{(1)} \quad \dot{\theta}_\nu^{(1)} = -\mathcal{H}\theta_\nu^{(1)} - \frac{3}{2}\frac{H_0^2\Omega_M}{a}\delta_M^{(1)} - c_s^2\nabla^2\delta_\nu^{(1)} \tag{3.47}$$

$$\dot{\delta}_\nu^{(2)} = -2\partial_j\nabla^{-2}\theta_\nu^{(1)}\partial_j\delta_\nu^{(1)} - 2\delta_\nu^{(1)}\theta_\nu^{(1)} - \theta_\nu^{(2)} \tag{3.48}$$

$$\begin{aligned}\dot{\theta}_\nu^{(2)} =& -\mathcal{H}\theta_\nu^{(2)} - 2\Big(\partial_i\partial_j\nabla^{-2}\theta_\nu^{(1)}\partial_i\partial_j\theta_\nu^{(1)}\Big) - 2\partial_j\nabla^{-2}\theta_\nu^{(1)}\partial_j\theta_\nu^{(1)} \\ &- \frac{3}{2}\frac{H_0^2\Omega_M}{a}\delta_M^{(2)} - c_s^2\nabla^2\delta_\nu^{(2)}\end{aligned} \tag{3.49}$$

5: See the appendix for derivation

combing these equations we were able to reduce it to one equation

$$\begin{aligned}\ddot{\delta}_\nu^{(2)} + \mathcal{H}\dot{\delta}_\nu^{(2)} = \frac{3}{2}\frac{H_0^2}{a}\Big(2\partial_j\nabla^{-2}\delta_M^{(1)}\partial_j\delta_\nu^{(1)} + 2\delta_\nu^{(1)}\delta_M^{(1)} + \delta_M^{(2)}\Big) \\ +c_s^2\Big(2\partial_j\delta_\nu^{(1)}\partial_j\delta_\nu^{(1)} + 2\delta_\nu^{(1)}\nabla^2\delta_\nu^{(1)} + \nabla^2\delta_\nu^{(2)}\Big) \\ +4\partial_j\nabla^{-2}\dot{\delta}_\nu^{(1)}\partial_j\dot{\delta}_\nu^{(1)} + 2\dot{\delta}_\nu^{(1)}\dot{\delta}_\nu^{(1)} + 2\partial_i\partial_j\nabla^{-2}\dot{\delta}_\nu^{(1)}\partial_i\partial_j\nabla^{-2}\dot{\delta}_\nu^{(1)}\end{aligned} \tag{3.50}$$

We were unable to move beyond this step. Instead, we focused on the neutrino equation.

3.6 Expanding on the neutrino equation

After having successfully derived and implemented eq. (3.44) we made attempts at simplifying it. So we tried to expand around the sound speed. Our reasoning for this was that we were under the belief that once the neutrino started to follow the dark matter, e.g. when the gravitational sourcing term in eq. (3.25) became dominant, the effective sound speed would become negligible. With this reasoning, we then expanded $M(a)$ (and thus the sound speed) around zero. Remembering the definition of $M(a)$

$$M(a) = 5\sqrt{\frac{\zeta(5)}{3\zeta(3)}}\Big(\frac{2kT_{\nu,0}}{m_\nu H_0\sqrt{a}}\Big) \tag{3.51}$$

expanding $M(a)$ around zero means $a \to \infty$. This gave[6]

$$\hat{\delta}_0 = c_1 + aD_0 - c_2 M - \frac{1}{2}M^2(c_1 - 2aD_0\gamma_{Euler} - 2aD_0\log(M)) + \mathcal{O}(M^3) \tag{3.52}$$

where the $\hat{\delta}_0$ represents the expansion around zero and γ_{Euler} is Eulers constant which is equal to 0.577.... We also tried to expand around the sound speed infinity, here the logic was to expand around the sound speed when it is the dominating term, so for $a \to 0$. This gave[7]

$$\hat{\delta}_\infty = 6\frac{aD_0}{M^2} + c_1\cos(M) + (-c_2 + \frac{\pi}{2}aD_0M^2)\sin(M) + \mathcal{O}(M^3) \tag{3.53}$$

where the $\hat{\delta}_0$ represents the expansion around infinity. Since we have that $M(a) \to \infty$ we should expect that the terms in cosine and sine in eq. (3.53) to oscillate very rapidly.

6: done in Mathematica
7: done in Mathematica

Chapter 4

Numerical Results

Before we begin we will give a brief description of CLASS, the code we used to compare and get initial values from.

4.1 CLASS

The "Cosmic Linear Anisotropy Solving System"[5] is a code designed to, amongst other things, numerically solve linear perturbations in cosmology. Like those of [11]. So for the neutrinos, the numerical solution is far more in-depth than our approximations. The code has many uses but the way we used CLASS was to

1. get initial values for our numerical solutions.
2. compare with our own numerical and analytical solutions.

We use the Python wrapper of CLASS which is available online[1].

4.2 Explanation

As explained in the introduction a lot of time was spent on numerical solutions of cold dark matter and neutrinos. This chapter will contain a walkthrough of what we did. All numerical solutions were done using the numerical differential equation solver in the Python package Scipy, using explicit Runge-Kutta method of order 5(4). As a comparison and source of the initial values, we used CLASS[5].

1: `https://github.com/lesgourg/class_public`

We also needed to choose cosmological parameters. For the ΛCDM runs we chose $H_0 = 68$ km/Mpc , $\Omega_M = 0.31$ and $\Omega_b = 0.05$ [6] and for the Einstein-de Sitter solutions we used $\Omega_M = 0.98$ and $\Omega_b = 0.05$. In addition, we also included a non-cold dark matter particle to represent the neutrinos, where we varied the mass to check the flexibility of our numerical solutions. Given that our goal was the neutrino density contrast δ_ν we did not focus on θ. One thing of note is that even though a gauge is not needed in the Newtonian limit, CLASS required us to either work in Newtonian or synchronous gauges. We worked with the synchronous gauge which meant that all the θ_{cdm} values were zero. The way around this was to use the combined 2nd order differential equations so that initial values for θ_{cdm} would not be necessary. The masses denoted on the figures are in eV. Finally, instead of sourcing from matter (baryons + CDM) we only sourced from CDM. Although sourcing from both would have been the more proper method, we only source from CDM for simplicity and to avoid errors.

4.3 Dark matter without neutrinos.

We began with numerically solving eq. (3.5) for different k values in ΛCDM and the Einstein-de Sitter Model. As can be seen in fig. 4.1 the solutions fit very well to those of CLASS. The best solutions were those in the Einstein-de Sitter model, while those in ΛCDM model were slightly larger for the higher k-values and slightly smaller for the very small k-values. But the behavior does fit very well.

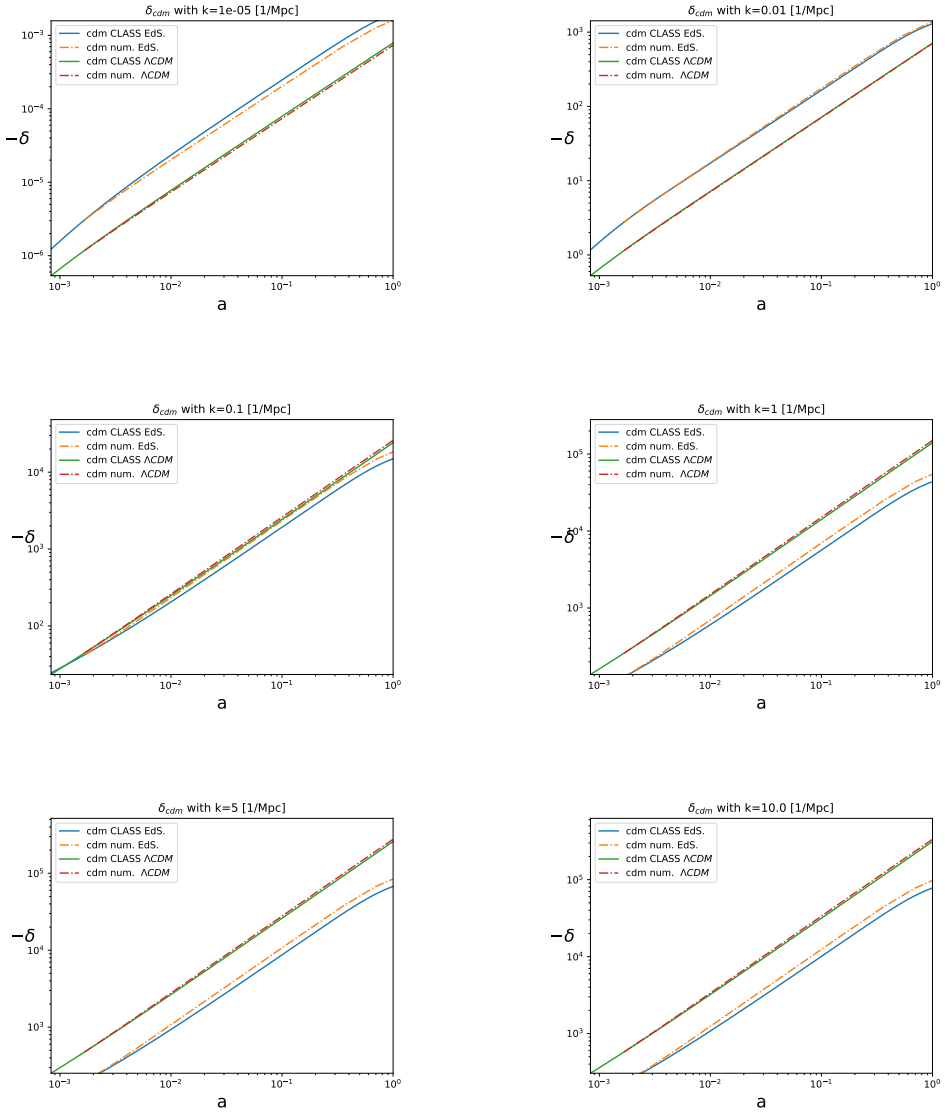

FIGURE 4.1: This figure shows the comparison between our numerical solution of eq. (3.5) and the solutions from CLASS in both ΛCDM and the Einstein-de Sitter Model with varying k. Our numerical solutions were initialized at $z = 600$..

As a way to check how well the numerical solutions worked compared to CLASS, as well as a step towards the bispectrum, we then created power spectra in both ΛCDM and in Einstein-de Sitter. This time we also varied the initial z value to illustrate its effect. As we can see on fig. 4.2 and fig. 4.3, our numerical power spectrum matches the behavior and scale of the power spectrum from CLASS. The numerical power spectrum in ΛCDM with $z_{ini} = 600$, (fig. 4.2), is the one that is the most of. The numerical solutions worked the best in the Einstein-de Sitter model and at z_{ini} $z = 100$(fig. 4.3), where is effectively a one-to-one overlap. This is not that surprising since the

Einstein-de Sitter model is the simpler model and with a lower z there is less time for errors to propagate. This is also in agreement with fig. 4.1 where the numerical ΛCDM was generally larger than the solution by CLASS.

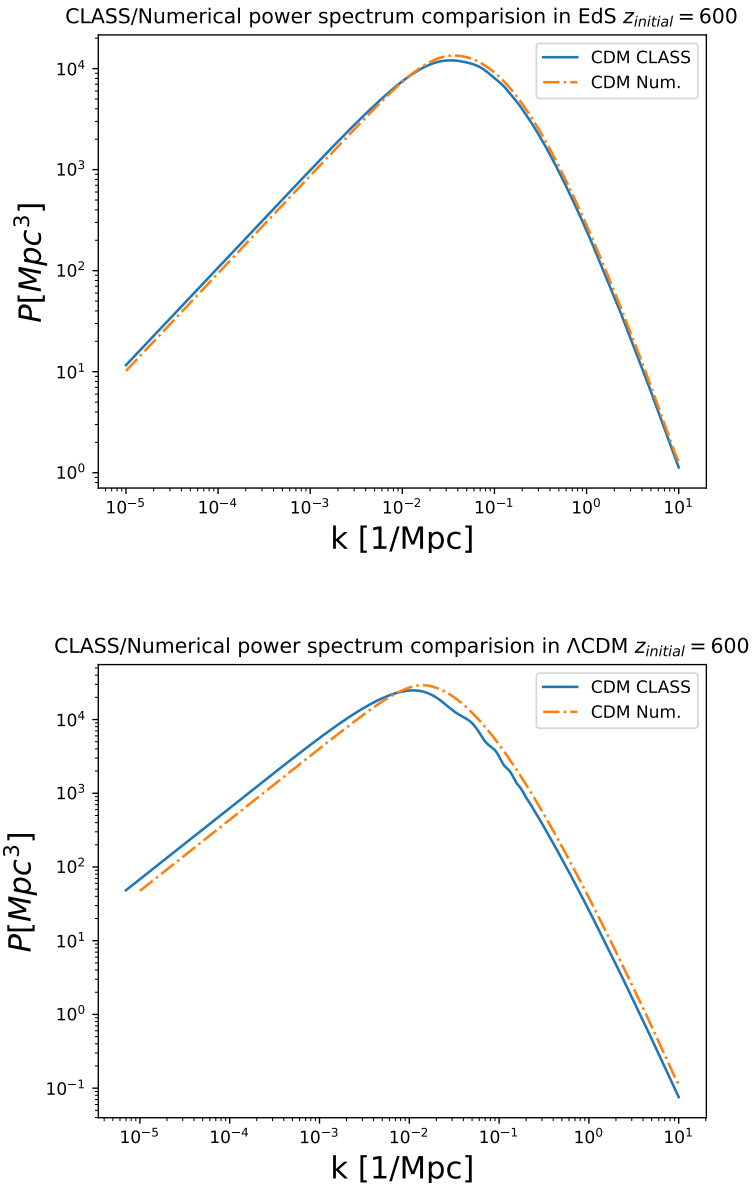

FIGURE 4.2: This figure shows the CDM power spectrum made using CLASS and the power spectrum that we made using our numerical solutions of eq. (3.4)in the ΛCDM and the Einstein-de Sitter model. initialized at $z = 600$.

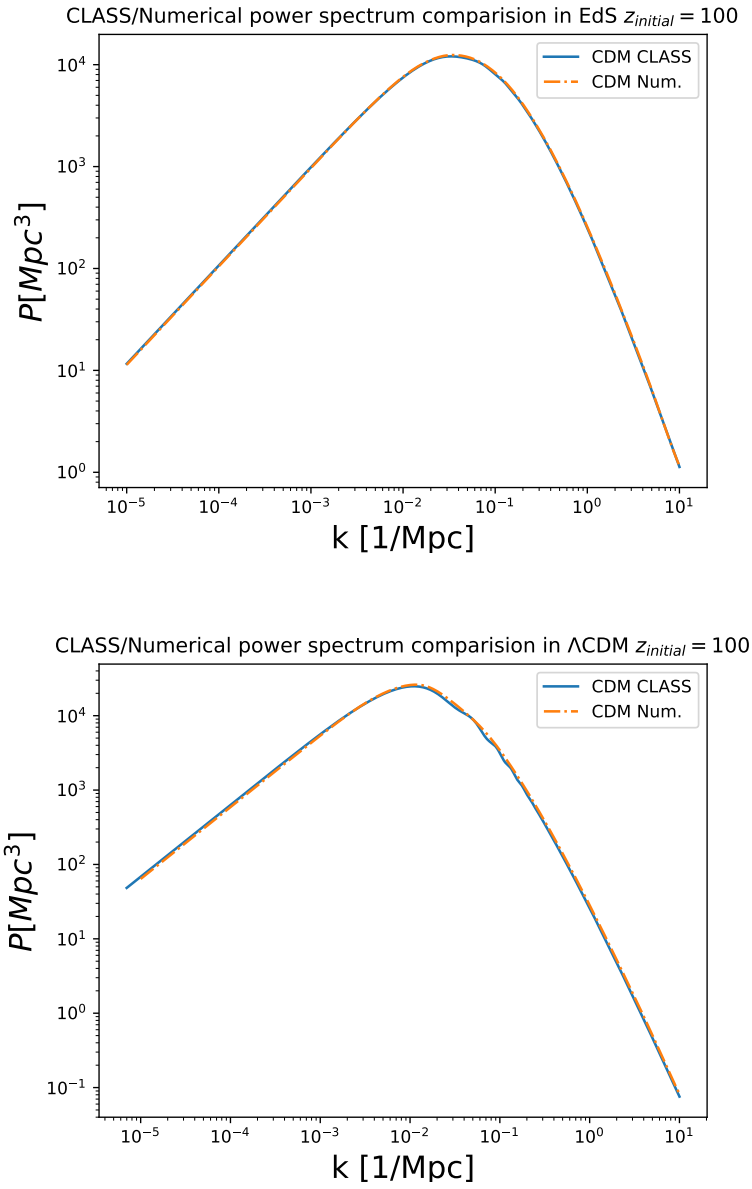

FIGURE 4.3: This figure shows the CDM power spectrum made using CLASS and the power spectrum that we made using our numerical solutions of eq. (3.4)in the ΛCDM and the Einstein-de Sitter model. initialized at $z = 100$.

4.4 Neutrinos

After working with the CDM power spectra we then began work on our approximate solutions to the neutrino perturbation equations. As explained in section 2.4.3 we used eq. (2.41) as an effective our sound speed which is approximately

$$c_s(a) \simeq 2.68 \frac{T_{\nu,0}}{m_\nu a} \tag{4.1}$$

This was our "theoretical" value for the effective sound speed but we did try other values to see if there was anything that might work better and to estimate the effect of the sound speed. We give the cases of using $\frac{2.68}{2}$ and 2 as comparisons to 2.68. We will refer to the factor in front of $\frac{T_{\nu,0}}{m_\nu a}$ as the "factor", "cs-factor" or "cs" and 2.68 as the "theoretical value".

Starting off, we have fig. 4.4 where we check for different k-values in both ΛCDM and Einstein-de Sitter. Although our numerical solutions are smaller than the solutions of CLASS, they do not follow the behavior of the CLASS solutions. Our numerical solutions also seem to stop their oscillating behavior later than the CLASS solutions. This is less of a problem for the low k-value $k = 0.1$.

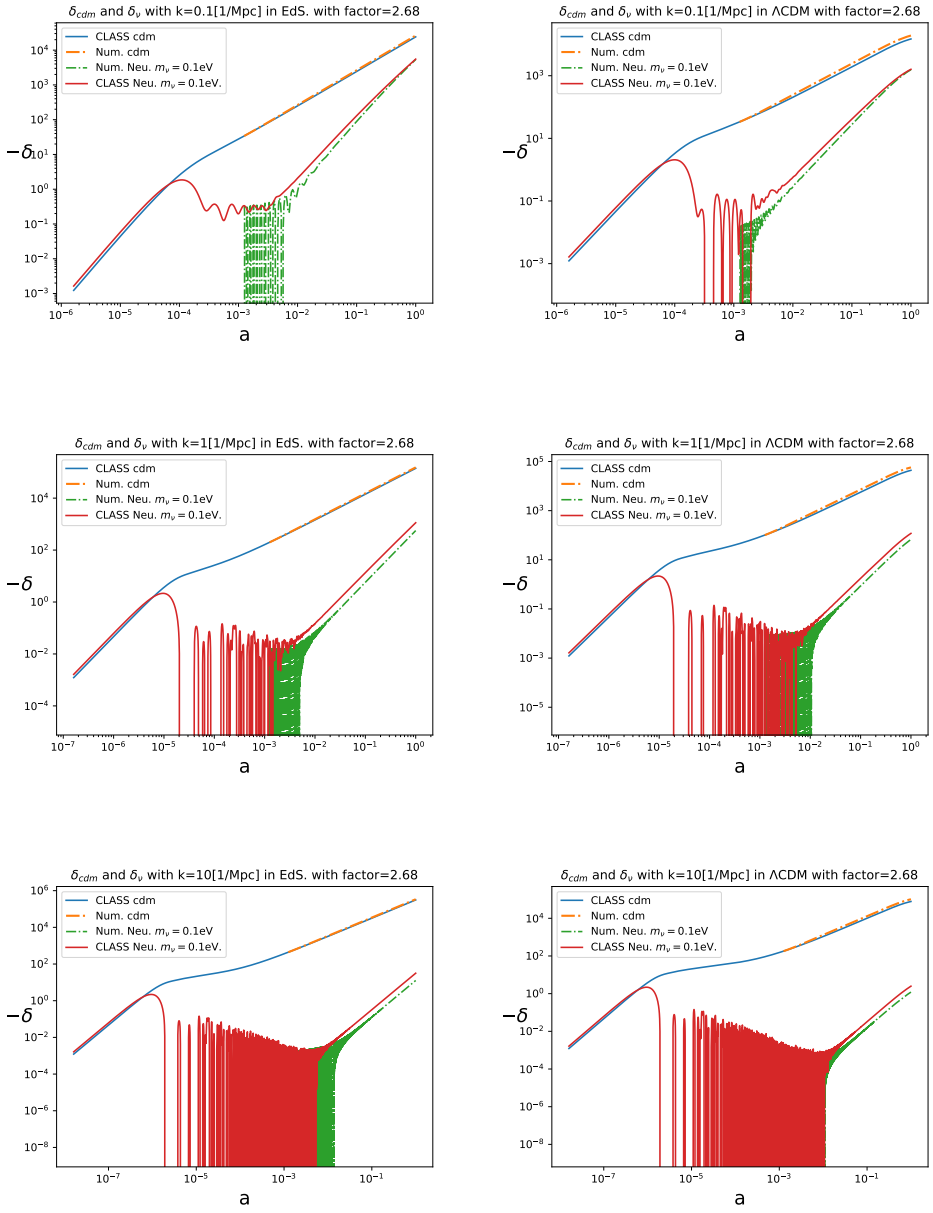

FIGURE 4.4: This figure shows the comparison between our numerical solution of eq. (3.5) and the solutions from CLASS with different k values, in the Einstein-de Sitter model and ΛCDM. Initialized at $z = 800$ where the factor=2.68 refers to what value was used as the factor in eq. (4.1)..

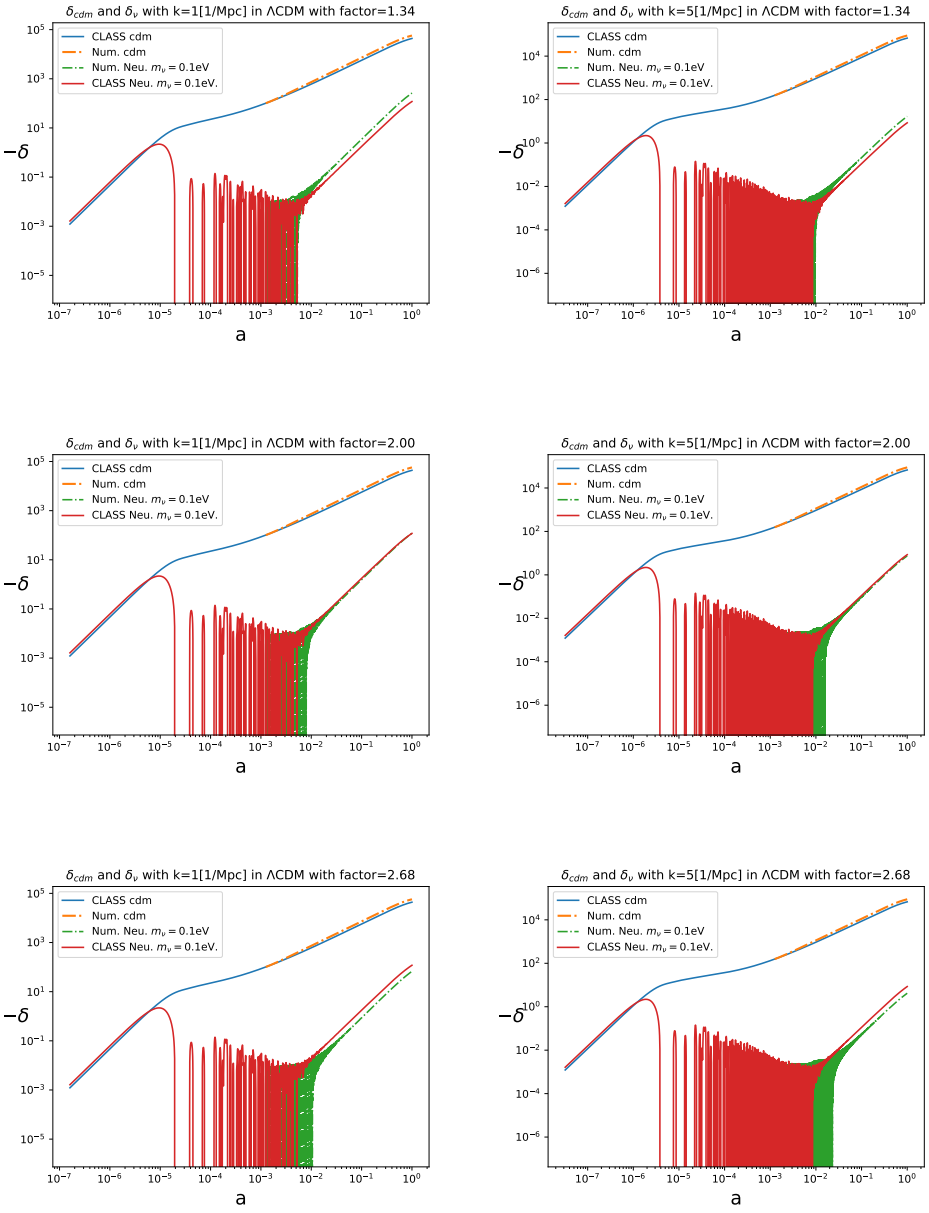

FIGURE 4.5: This figure shows the effect of altering the factor in eq. (4.1). Our numerical solutions of eq. (3.4) are compared with the solutions from CLASS. Or numerical solutions were initialized at $z = 600$..

In fig. 4.5 we vary the cs-factor and the k-values. We observe that the subfigures with a cs-factor of 1.34 essentially have the opposite problem of the theoretical value in that they are slightly larger than the CLASS solutions. Interestingly in the subfigures with $cs = 2$ our solutions line up better with the solutions of CLASS than the numerical solutions that use the theoretical value.

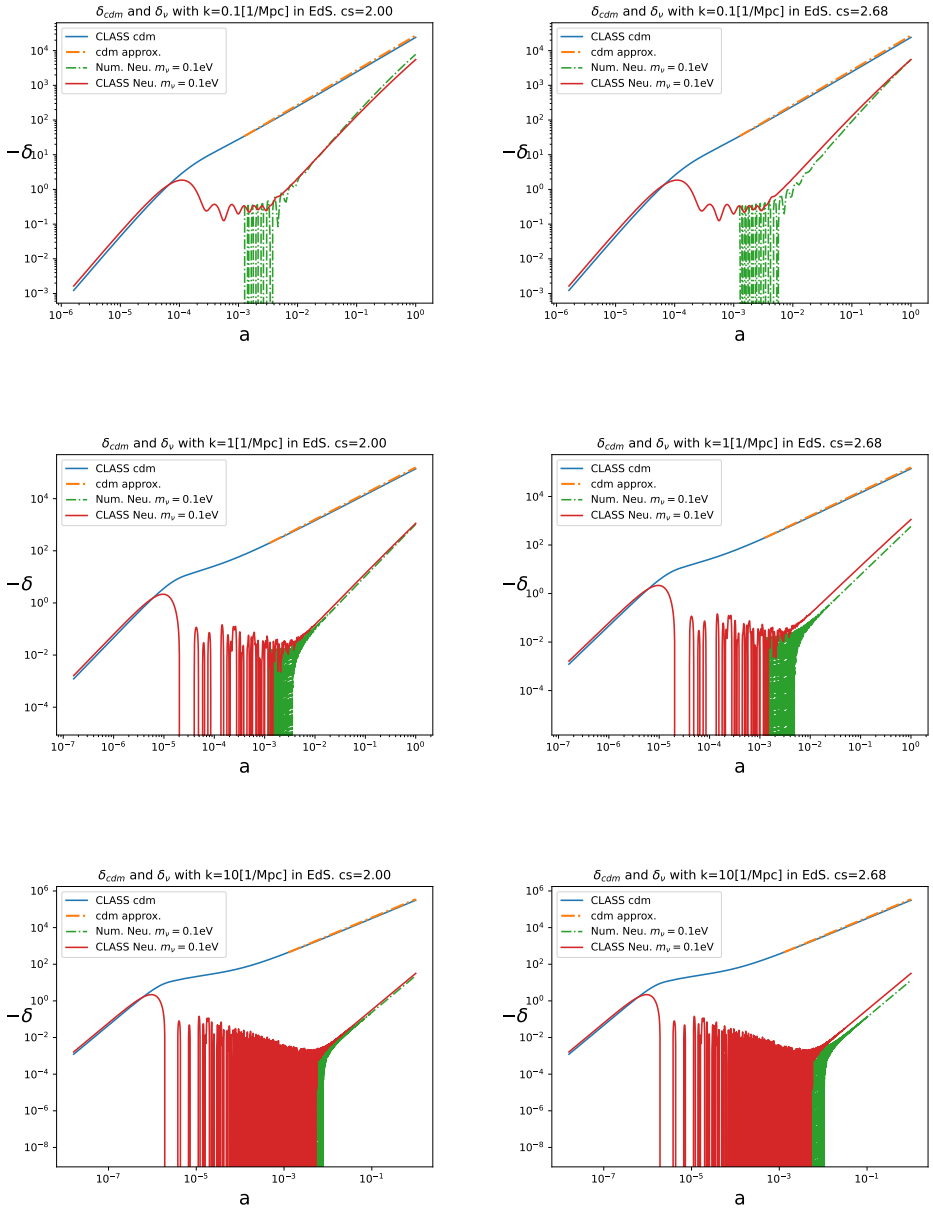

FIGURE 4.6: This figure is a follow up on figure fig. 4.5. Here we show the difference in using $cs = 2.00$ and $cs = 2.68$ as the front factors in eq. (4.1) for different k-values. Unlike fig. 4.5 these solutions are in the Einstein-de Sitter model. Our numerical solutions are compared with the solutions of CLASS, additionally, we use eq. (3.22) as the gravitational source for the neutrinos in our solution. Our solutions were initialized at $z = 800$..

Expanding on fig. 4.5 we have fig. 4.6 where we compare our solutions with a cs factor of 2 with solutions that use the theoretical value. Again we see that the solution with $cs = 2$ lines up better with the solutions of CLASS than our numerical solutions that use the theoretical value. Both the solutions that

use $cs = 2$ and the ones that use the theoretical value end their oscillating behavior later than the solutions of CLASS do. In this figure, we use eq. (3.22) as a gravitational source for our neutrinos (instead of numerically solving for the CDM as well) and it would appear to work quite well.

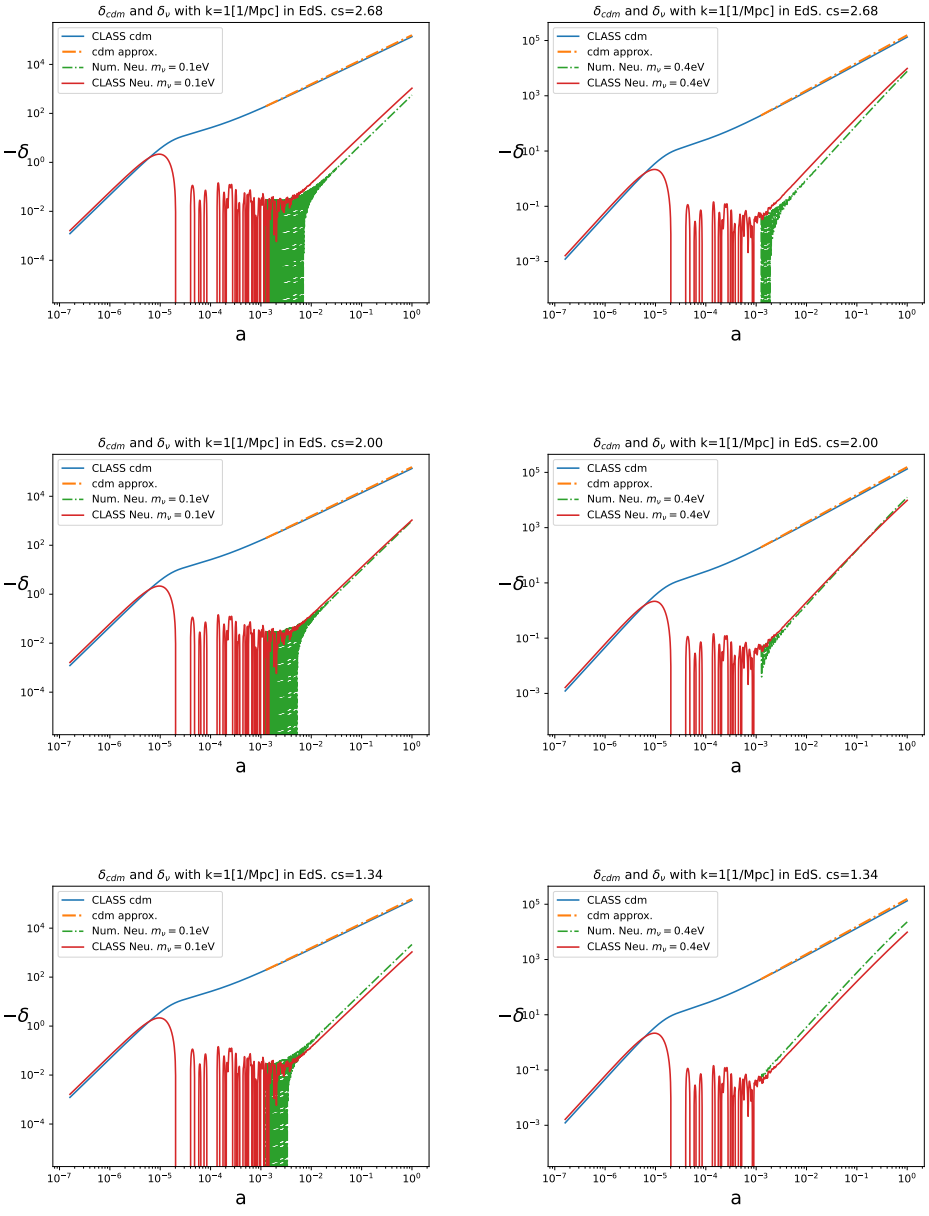

FIGURE 4.7: In these figures we vary the factor in eq. (4.1) like in fig. 4.5. Our numerical solutions are in the Einstein-de Sitter model and compared with those of CLASS. Our solutions are initialized at $z = 800$. .

In fig. 4.7 we vary the mass of the neutrino and use different cs-factors. The solutions that use a higher neutrino mass end their oscillating behavior

earlier which makes sense since the effective sound speed term is inversely proportional to the neutrino mass. Despite the change in the neutrino mass the solutions that use $cs = 2$ still line up better with the solutions of CLASS than the solutions that use the theoretical value.

4.5 Neutrino power spectrum

Repeating the steps of the CDM-only solutions, we generated power spectra for the neutrinos in fig. 4.8, where we varied the effective sound speed factor. In general, we see that the numerical solutions of the neutrinos do follow the behavior of CLASS, however, we again note a clear difference between the power spectrum that used 1.34 as a factor and those that did not. The power spectrum that used 1.34 is off and while the power spectra are virtually identical for k-values below 10^{-2} 1.34 is consistently off for k-values above 10^{-2}, although the general behavior is still similar to that of the power spectrum form CLASS. Meanwhile for the power spectrum, which uses a cs-factor of 2, and the power spectrum, which uses the theoretical value of 2.68, an interesting pattern emerges. It would appear that the solutions which use 2 are better for higher values of k while the solutions that use the theoretical value fit better to the solutions by CLASS $k < 0.1$ when $m_\nu = 0.1$eV and $k < 0.3$ when $m_\nu = 0.4$eV .

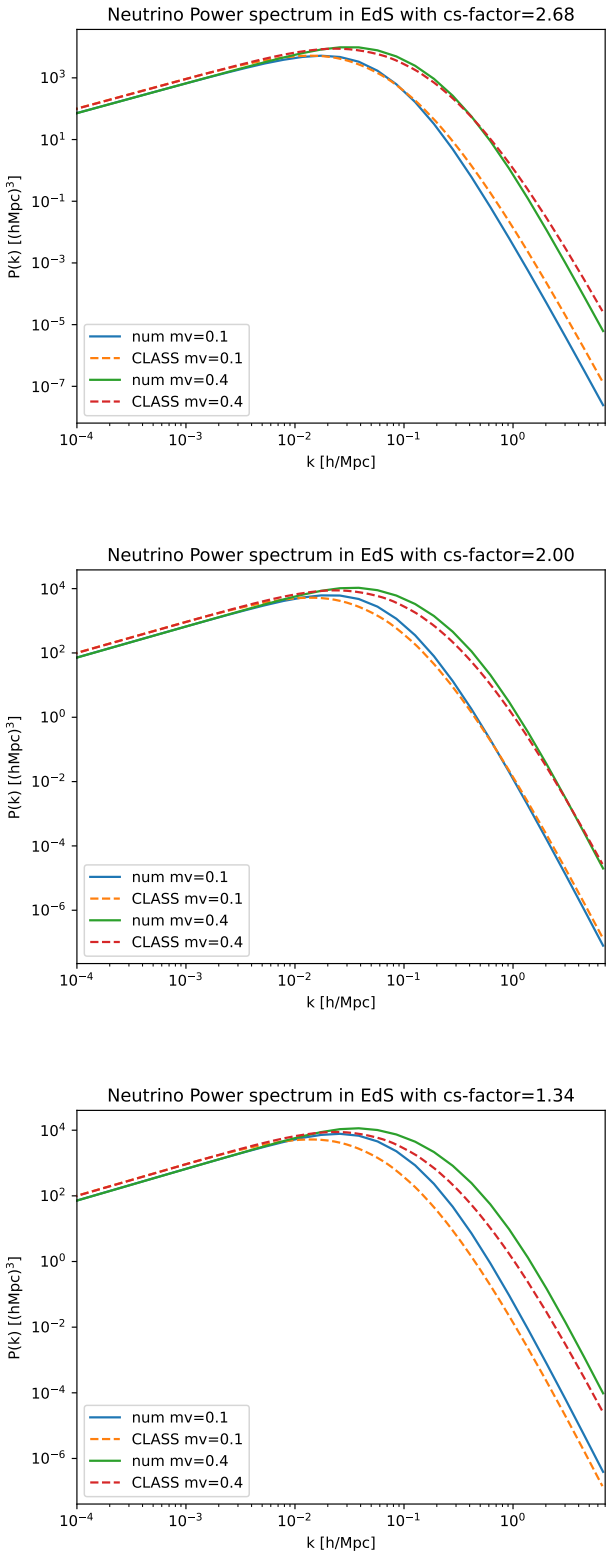

FIGURE 4.8: The neutrino power spectra for Neutrinos with different mass and using different factors in eq. (4.1). Our numerical solutions are compared with those of CLASS and were initialized at $z = 800$..

This marked the end of us working in the ΛCDM model. This is a result of us now using the equation which assumes in Einstein-de Sitter.

4.6 Neutrino equation

Having shown the numerical part of this thesis we now turn to the Neutrino equation of eq. (3.44). In fig. 4.9 and fig. 4.10 we see how well the equation works when compared to both CLASS and the numerical solutions of the previous figures, where we vary the mass and k values. We note first how well the equation actually works when compared with the numerical solutions. In fact, the equation fits so well that there are several figures in fig. 4.9 and fig. 4.10 where we can barely see the numerical solution because it is covered over by the equation. We can see that for the lower $k-$value 0.1 in fig. 4.10 the equation does appear to be slightly out of phase with the numerical solutions. However, this does not seem to have a serious effect on the equations as they still follow the numerical closely. Like in the previous figures where the cs factor was set to 2 the equation in fig. 4.9 matches the solutions from CLASS better than when the theoretical value was used like, in fig. 4.10.

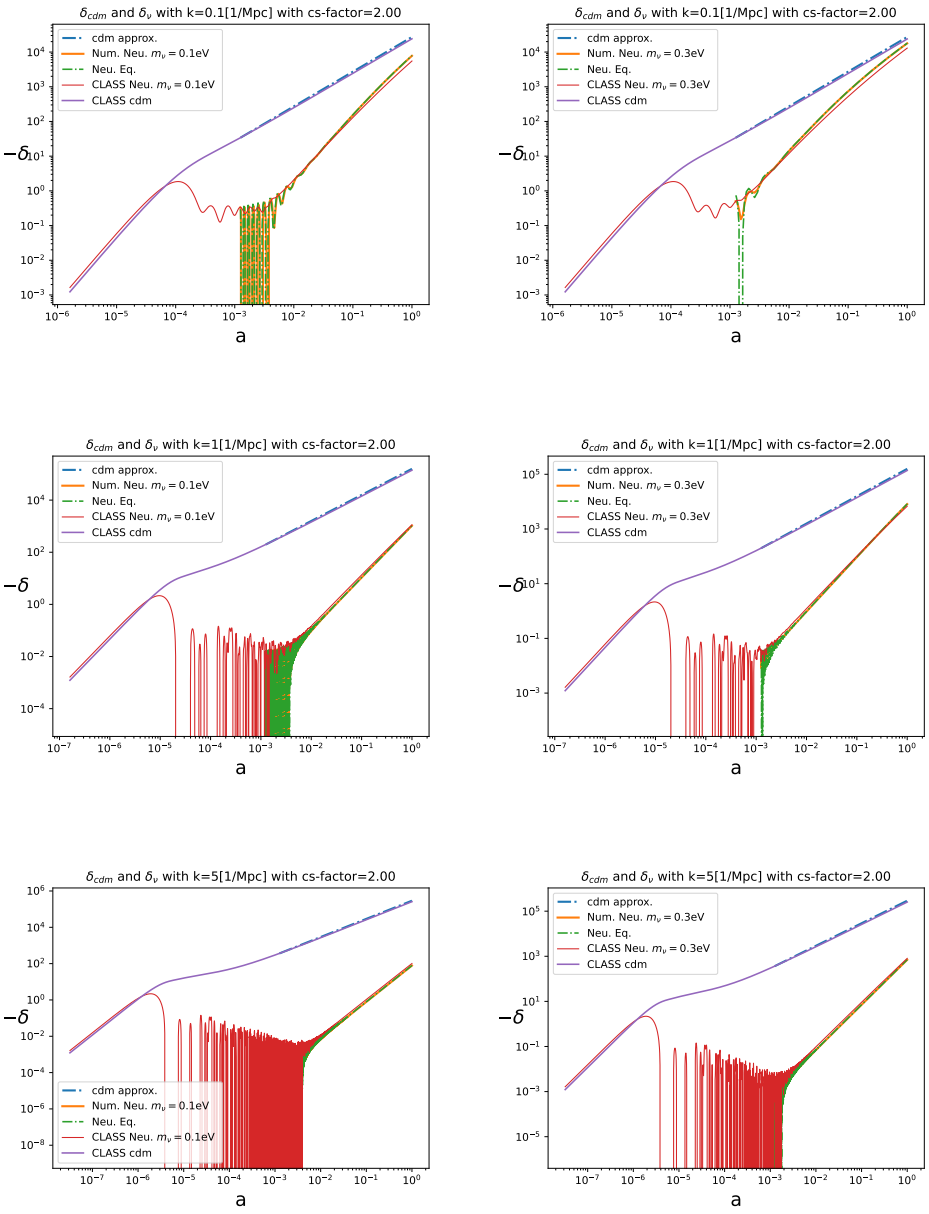

FIGURE 4.9: This figure shows our numerical solutions, our Neutrino equation, and the solutions of CLASS, where we vary the mass and the k values and we have set the factor of eq. (4.1) to 2. This figure is best compared with fig. 4.10 where we have set the sound speed strength to that of eq. (4.1) .

4.6.1 Power spectra

We tested the effectiveness of eq. (3.44) by making power spectra, in fig. 4.11 where we have again varied the factor of the neutrino sound speed. fig. 4.11 is almost identical to that of fig. 4.8, this is not surprising as eq. (3.44) is a solution to the equations that were used in fig. 4.8.

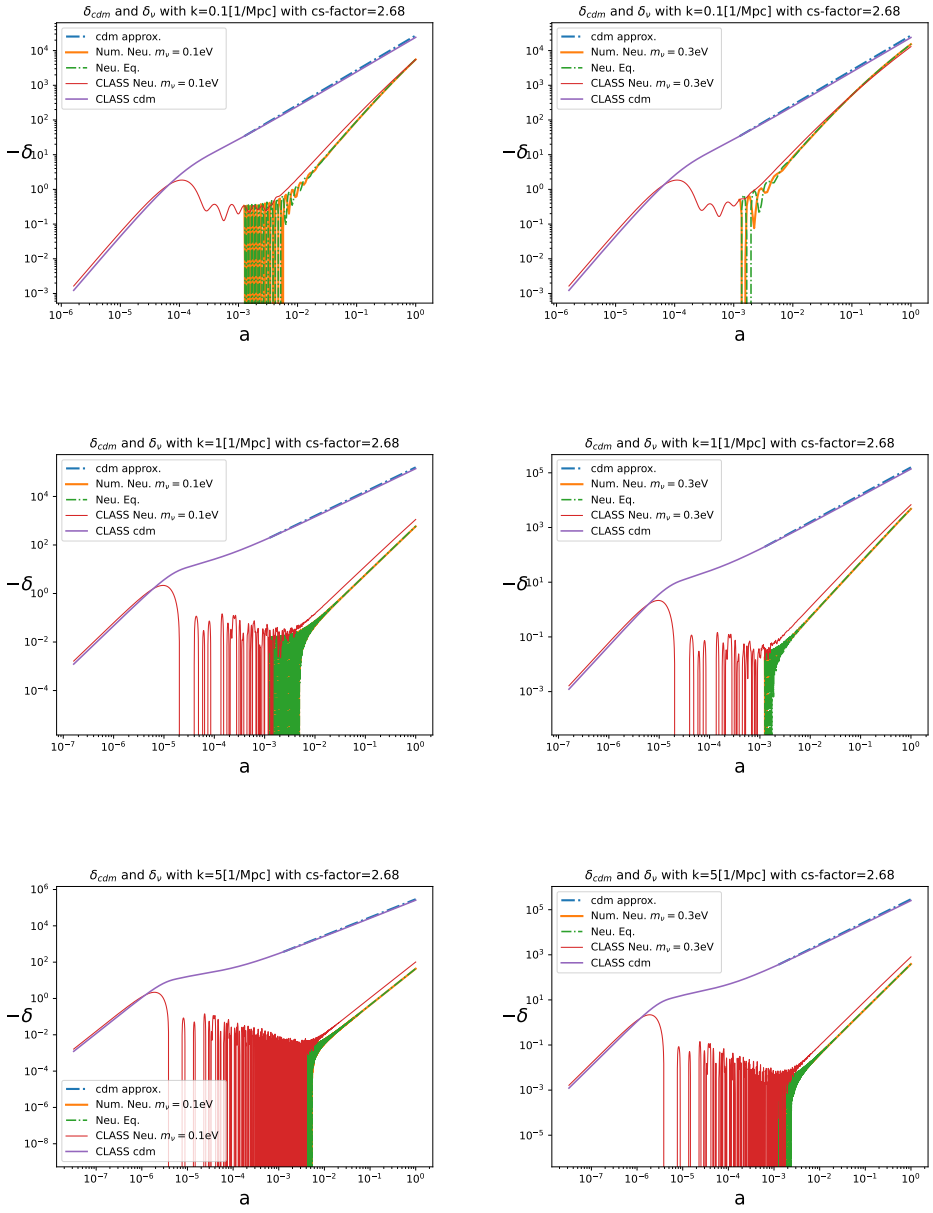

FIGURE 4.10: This figure shows our numerical solutions, our Neutrino equation, and the solutions of CLASS, where we vary the mass and the k values and we have set the factor of eq. (4.1) to 2.68. This figure is best compared with fig. 4.9 where we have set the factor to 2..

4.7 Bispectrum

As stated before, we did not succeed with the bispectrum. However, we did attempt, out of curiosity to replicate the Neutrino equilateral bispectrum using the CDM kernel. The idea was based on the observation that the solutions to the neutrino perturbations start to move towards CDM after the oscillations

end and so we hypothesized that the neutrino and CDM bispectrum might be similar to one another. fig. 4.12 is our attempt at generating an equilateral reduced CDM bispectrum in Einstein-de Sitter. The reduced bispectrum is given as

$$Q(k_1, k_2, k_3) = \frac{B(k_1, k_2, k_3}{P(k_1)P(k_2) + P(k_1)P(k_3) + P(k_2)P(k_3)}. \tag{4.2}$$

Equilateral means that all the k are of equal length. We used the parameterization $k_2 = tk_1$ and $k_3 = \sqrt{k_1^2 + k_2^2 - 2\cos\theta k_1 k_2}$, which then gave us fig. 4.12, which fits well with the reduced equilateral bispectra in [17].
fig. 4.13 shows our attempt at combing neutrino power spectra generated using our equation and the CDM kernel eq. (3.11). The general behaviors are similar to those in [17]. However, since we did work a lot with this hybrid bispectrum we are unable to clearly state how well it works. it is not clear to us how well it worked and further work is required.

4.8 Approximations to the Neutrino equation

As explained in section 3.6 we attempted to approximate the neutrino equation eq. (3.44), where we expanded the sound speed around zero and infinity. The success of these may be seen in fig. 4.14. The expansion around zero works well for $a >> 1$ and the expansion around infinity works well for $a \leq 1$. This suggests that the sound speed is still relevant for some time after the neutrino density perturbations have stopped oscillating.
In fig. 4.15 we have plotted the rations between the expansions and the equation to better visualize when the expansions work well using two different cs-factors. We notice that when using the theoretical cs-factor the expansion around infinity is better than when using the cs-factor of 2 and the reverse is the case for the expansion around zero.

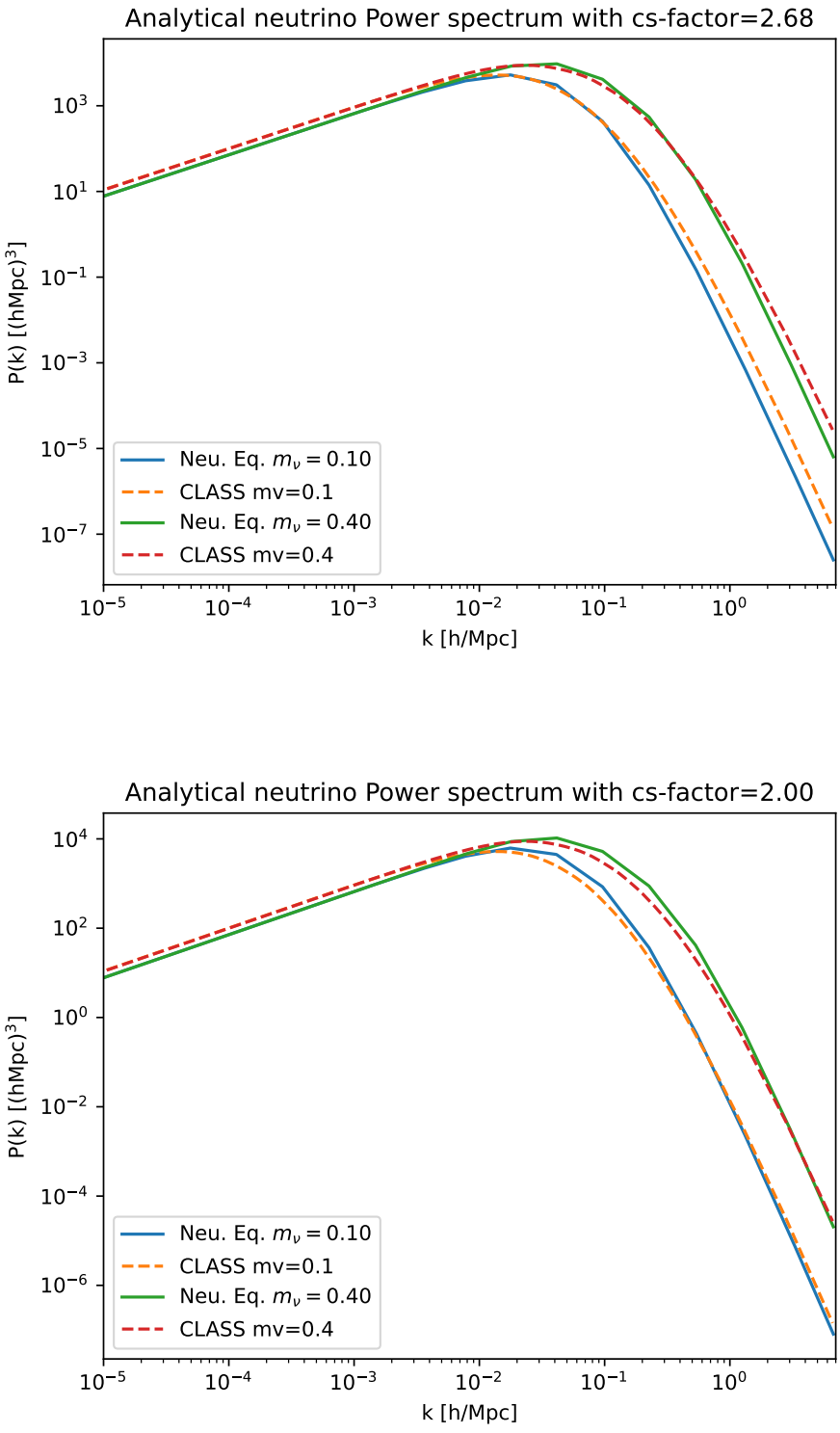

FIGURE 4.11: A comparison of Neutrino power spectra using different neutrino mass and factors, where we have used our neutrino equation to generate the power spectra and compared them with the power spectrum from CLASS..

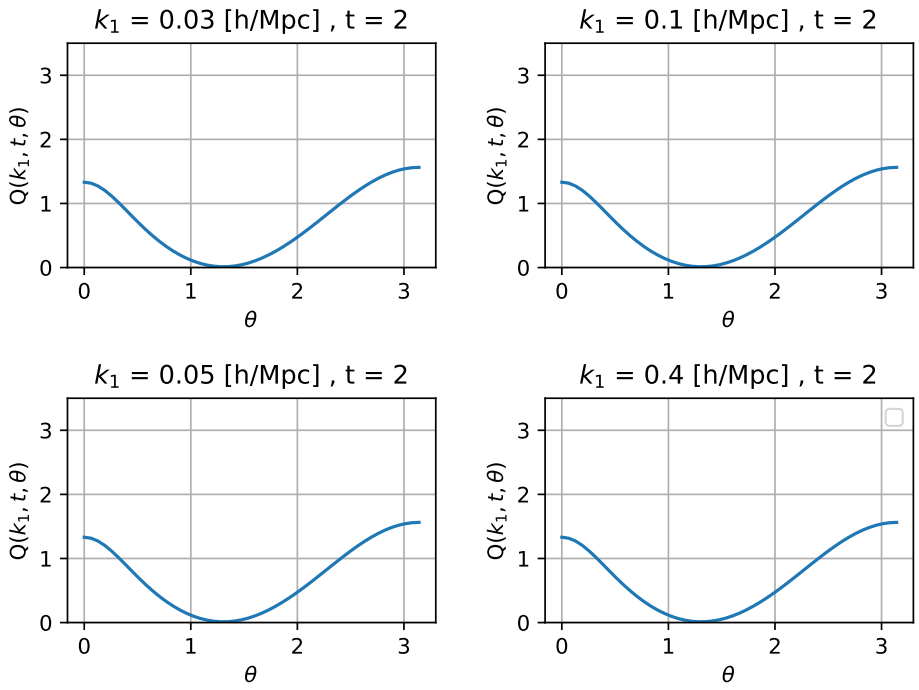

FIGURE 4.12: The CDM Equilateral bispectrum in the Einstein-de Sitter model.

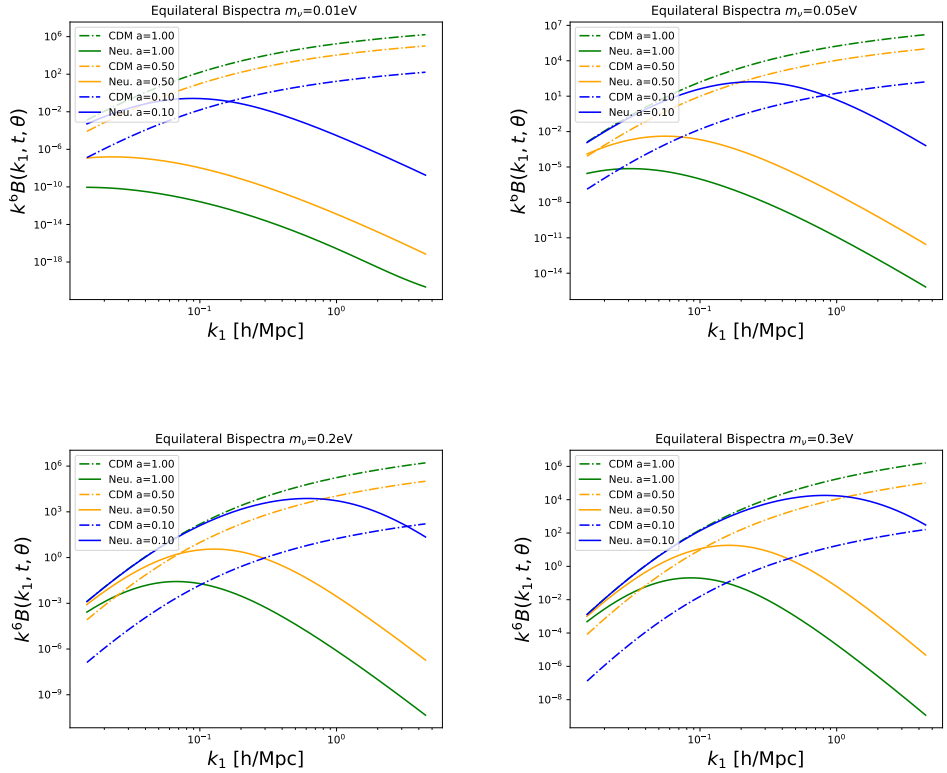

FIGURE 4.13: Neutrino/CDM bispectra using the CDM approximation from eq. (3.22) with a sound speed factor of 2.68 in the Einstein-de Sitter model. Depicted are the Bispectra for CDM and the bispectrum where we use the CDM kernel from eq. (3.11) on the neutrino $\delta^{(1)}$ at different a.

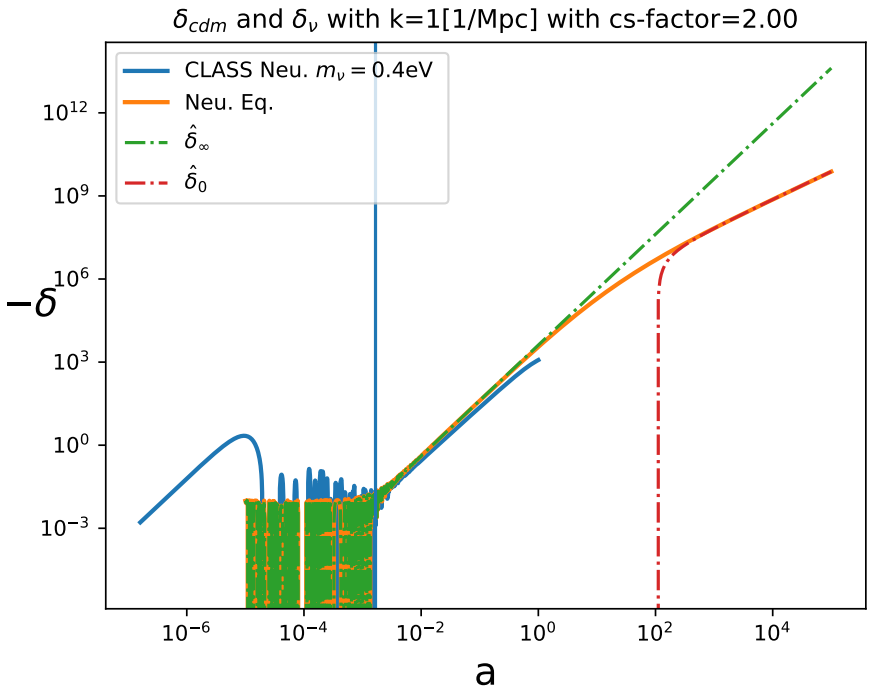

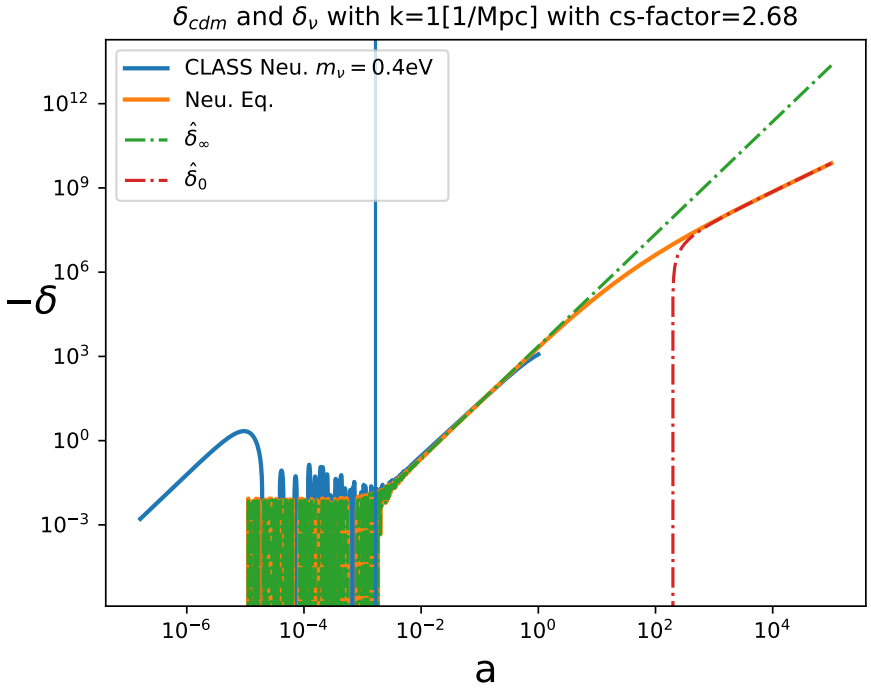

FIGURE 4.14: These figures show our expansions of the sound speed around zero and infinity (eq. (3.52) and eq. (3.53)), compared with our neutrino equation and the numerical solutions from CLASS with two different sound speed factors. Using the notation of eq. (3.52) and eq. (3.53) the index represents which value was expanded around. The neutrino equation was initialized at $z = 600$. Unlike the previous figures we have here chosen to go far beyond $a = 1$.

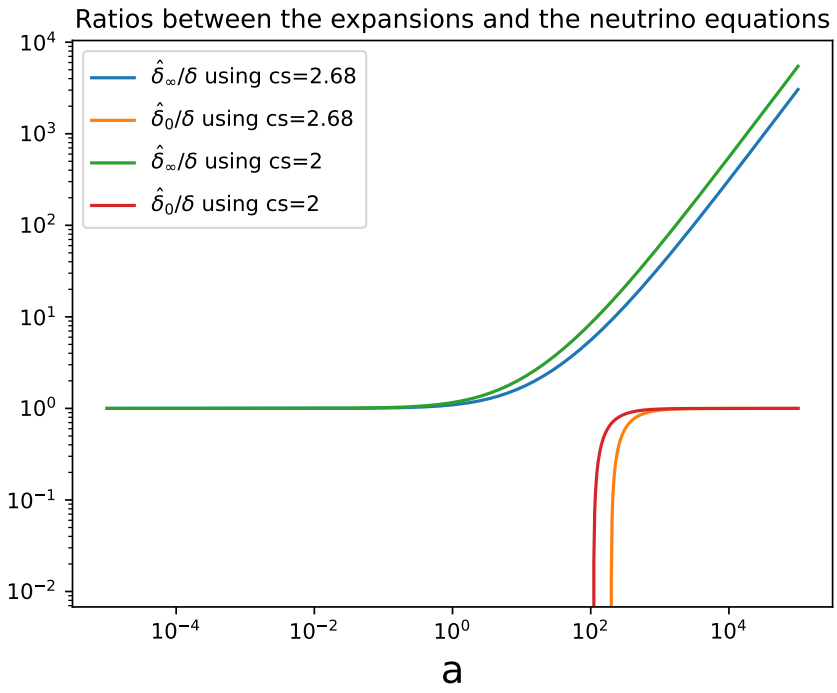

FIGURE 4.15: This figure depicts the ratio between the neutrino equation and the two expansions that we made around zero and infinity using 2 different cs-factors, k=1 and $m_\nu = 0.40$eV initialized at $z = 600$.

Chapter 5

Discussion

We can see from the figures that our numerical solutions worked. We were able to numerically solve the equations for the CDM and neutrinos in both ΛCDM and the Einstein-de Sitter model. Although the ΛCDM solutions do work well, the Einstein-de Sitter solutions were in general better. This is not surprising when one considers that the Einstein-de Sitter model is a simpler model than ΛCDM and we should thus not be surprised when the numerical solutions work better. As stated previously we used the synchronous gauge. We were thus required to work around the problem that θ_{cdm} was constantly zero. we did this by using the combined differential equations where θ was replaced $\dot{\delta}$. Instead we approximated the derivative of δ by using an interpolated version of δ using "scipy.interpolate.interp1d" so we could make

$$\dot{\delta}_{approx} = \frac{\delta(a_0 + h/2) - \delta(a_0 - h/2)}{h} \tag{5.1}$$

where h was set to a low value and a_0 was the starting point of the numerical solution. This appears to have worked. It is worth noting that even without this method and instead using θ from CLASS so $\dot{\delta}(a_0) = -\theta(a_0) = 0$, the numerical solution would still work although it would lag behind CLASS' solutions by some offset. In eq. (3.44) there is a $\dot{\delta}_\nu(a_0)$ dependent term, however, we found no issue in setting this to zero. Our rationale for this was that since for all our z_{ini} value (usually 600, but a few times we used 800), the neutrinos were still oscillating very intensively, the derivative at a specific z_{ini} could thus be approximated to be at a peak of an oscillation as these oscillations were so rapid and so $\delta_\nu \simeq 0$. As stated it worked, with no issue, we did also test with eq. (5.1) but that had no noticeable effect.

The power spectra were a very useful way for us to check the success of the numerical and analytical solutions. Unsurprisingly the best power spectra were in fig. 4.3 which was also the most simplistic, as it was initialized only

at $z_{init} = 100$ and using the Einstein-de Sitter model. So simpler equations and with less time for errors to propagate. Meanwhile, the neutrino power spectra that used a sound speed factor of 1.34 was the most off from the power spectrum of CLASS when compared with all other power spectra, but it did still follow the behavior of CLASS. But the more interesting ones were those of fig. 4.8 and fig. 4.11 where we varied the neutrino sound speed factor. As stated the power spectrum where the sound speed factor was set to 1.34 was the one that was the most off as compared with CLASS. But interestingly it is not clear whether the values 2 or 2.68 is the better. Based on (fig. 4.5, fig. 4.6, fig. 4.7, and fig. 4.9) one might assume that 2.68 would not be the best as 2.00 lines up better with the CLASS solution. However, it would appear that the equation slightly underperforms for higher values of k when using 2.00 while the equation slightly overperforms when using 2.68 as seen in fig. 4.8 and fig. 4.11. This might suggest that neither 2.68 nor 2.00 are optimal values and we should note that we simply pick 2 as an example. Finding a numerically optimal sound speed factor would thus be a clear next step forward.

The equation works. It is in fact quite remarkable how well it works. We did not initially assume that using the sound speed method for the neutrinos to account for their oscillation, to replicate CLASS' solution would do as well as it did. Deriving the equation was of cause only possible because of the δ_{CDM} in Einstein-de Sitter eq. (3.22) which we called the approximation for simplicity. It fits quite well with the solutions of CLASS. It is worth noting that like our numerical solutions, the equation did not stop oscillation until a bit after the solutions of CLASS.

Of high interest is the expansions. Initially, we believed that the expansion around zero would be the logical choice as we believed the sound speed to be negligible after the neutrinos perturbations stopped oscillating, but that is apparently not the case. fig. 4.14 illustrates that the expansions around zero only work for high values of a ($a >> 1$). Meanwhile, the expansion around infinite worked surprisingly well although it did start to break down at around $a \simeq 1$. Rigorously testing the limits of these expansions was not something that we did, although it would be a clear next step to check just how well these expansions work.

Finally, we have the bispectrum. On this front the results are mixed, we failed to derive an analytical neutrino bispectrum however our hybrid bispectrum fig. 4.13 does seem to replicate some of the behavior of the neutrino bispectrum in [17]. Further work is needed.

Chapter 6

Conclusion

To conclude, we derived an analytical equation that describes the neutrino density perturbations eq. (3.44). Our analysis shows that the value of the effective sound speed from [1] is not completely optimal, although it does work. We showed two expansions to the equation eqs. (3.52) and (3.53) that work well for $a < 1$ and $a >> 1$. The success of the expansion suggests that the sound speed term remains relevant for approximating the behavior of the neutrino perturbations for much longer than we initially realized. We did not succeed with the neutrino bispectrum but our test of our matter-neutrino hybrid bispectrum does show some promise and may thus be of further interest.

Bibliography

[1] Masatoshi Shoji and Eiichiro Komatsu. 'Massive neutrinos in cosmology: Analytic solutions and fluid approximation'. In: *Phys. Rev. D* 81 (12 June 2010), p. 123516. URL: https://link.aps.org/doi/10.1103/PhysRevD.81.123516.

[2] Scott Dodelson and Fabian Schmidt. *Modern Cosmology*. Second Edition. Academic Press. URL: https://www.sciencedirect.com/science/article/pii/B9780128159484000061.

[3] Brian R. Martin and Graham Shaw. *Nuclear and Particle Physics*. Wiley, 2019. URL: https://www.wiley.com/en-us/Nuclear+and+Particle+Physics%5C%3A+An+Introduction%5C%2C+3rd+Edition-p-9781119344612.

[4] Thomas Tram et al. 'The intrinsic matter bispectrum in ΛCDM'. In: *Journal of Cosmology and Astroparticle Physics* 2016.05 (May 2016), p. 058. URL: https://dx.doi.org/10.1088/1475-7516/2016/05/058.

[5] Diego Blas, Julien Lesgourgues and Thomas Tram. 'The Cosmic Linear Anisotropy Solving System (CLASS). Part II: Approximation schemes'. In: *Journal of Cosmology and Astroparticle Physics* 2011.07 (July 2011), pp. 034–034. URL: https://doi.org/10.1088%5C%2F1475-7516%5C%2F2011%5C%2F07%5C%2F034.

[6] Barbara Ryden. *Introduction to Cosmology*. 2nd ed. Cambridge University Press, 2016.

[7] Michael Duerr and Pavel Fileviez Pérez. 'Baryonic dark matter'. In: *Physics Letters B* 732 (May 2014), pp. 101–104. URL: https://doi.org/10.1016%5C%2Fj.physletb.2014.03.011.

[8] Planck Collaboration: N. Aghanim et al. 'iPlanck/i2018 results'. In: *Astronomy &amp Astrophysics* 641 (Sept. 2020), A6. URL: https://doi.org/10.1051%5C%2F0004-6361%5C%2F201833910.

[9] Adam G. Riess et al. 'Cosmic Distances Calibrated to 1% Precision with Gaia EDR3 Parallaxes and Hubble Space Telescope Photometry of 75 Milky Way Cepheids Confirm Tension with Λ*CDM*'. In:

The Astrophysical Journal Letters 908.1 (Feb. 2021), p. L6. URL: https://doi.org/10.3847%5C%2F2041-8213%5C%2Fabdbaf.

[10] Sean M. Carroll. *Spacetime and Geometry An Introduction to General Relativity*. Cambridge University Press. URL: https://www.cambridge.org/highereducation/books/spacetime-and-geometry/38EDABF9E2BADCE6FBCF2B22DC12BFFE#overview.

[11] Chung-Pei Ma and Edmund Bertschinger. 'Cosmological Perturbation Theory in the Synchronous and Conformal Newtonian Gauges'. In: *The Astrophysical Journal* 455 (Dec. 1995), p. 7. URL: https://doi.org/10.1086%5C%2F176550.

[12] E. Kolb and M. Turner. *The Early Universe*. Frontiers in physics. Avalon Publishing, 1994.

[13] F. Bernardeau, S. Colombi, E. Gaztañaga and R. Scoccimarro. 'Large-scale structure of the Universe and cosmological perturbation theory'. In: *Physics Reports* 367.1-3 (Sept. 2002), pp. 1–248. URL: https://www.sciencedirect.com/science/article/pii/S0370157302001357?via%5C%3Dihub.

[14] Guido Walter Pettinari. *The Intrinsic Bispectrum of the Cosmic Microwave Background*. Springer International Publishing, 2016. URL: https://doi.org/10.1007%5C%2F978-3-319-21882-3.

[15] Jeppe Dakin, Jacob Brandbyge, Steen Hannestad, Troels HaugbØlle and Thomas Tram. 'νCOiN/iCEPT: cosmological neutrino simulations from the non-linear Boltzmann hierarchy'. In: *Journal of Cosmology and Astroparticle Physics* 2019.02 (Feb. 2019), pp. 052–052. URL: https://iopscience.iop.org/article/10.1088/1475-7516/2019/02/052.

[16] M. Zennaro et al. 'Initial conditions for accurate N-body simulations of massive neutrino cosmologies'. In: *Monthly Notices of the Royal Astronomical Society* 466.3 (Dec. 2016), pp. 3244–3258. URL: https://doi.org/10.1093/mnras/stw3340.

[17] Johan Kølsen de Wit. 'Using the Bispectrum of Density Fluctuations to Probe Cosmic Structure'. Unpublished. Master's thesis. University of Aarhus, 2022.

Appendix A

Analytical results

A.1 rewriting eq. (3.19) to eq. (3.20)

$$\ddot{D} + \frac{2}{\tau}\dot{D} = \frac{6}{\tau^2}D \tag{A.1}$$

$$\frac{\mathrm{d}}{\mathrm{d}\tau} = \frac{\mathrm{d}}{\mathrm{d}\tau}\frac{\mathrm{d}a}{\mathrm{d}a} = \frac{\mathrm{d}a}{\mathrm{d}\tau}\frac{\mathrm{d}}{\mathrm{d}a} = a\mathcal{H}\frac{\mathrm{d}}{\mathrm{d}a} = H_0\sqrt{a}\frac{\mathrm{d}}{\mathrm{d}a} \tag{A.2}$$

$$\ddot{D} = \frac{\mathrm{d}^2}{\mathrm{d}\tau^2}D = \frac{\mathrm{d}}{\mathrm{d}\tau}\Big(\frac{\mathrm{d}}{\mathrm{d}\tau}D\Big) = H_0\sqrt{a}\frac{\mathrm{d}}{\mathrm{d}a}\Big(H_0\sqrt{a}\frac{\mathrm{d}}{\mathrm{d}a}D\Big) \tag{A.3}$$

$$H_0\sqrt{a}H_0\Big(\frac{\mathrm{d}\sqrt{a}}{\mathrm{d}a}\frac{\mathrm{d}}{\mathrm{d}a}D + \sqrt{a}\frac{\mathrm{d}^2}{\mathrm{d}a^2}D\Big) = \sqrt{a}H_0^2\Big(\frac{1}{2\sqrt{a}}\dot{D}_a + \sqrt{a}\ddot{D}_a\Big) \tag{A.4}$$

$$\ddot{D} = H_0^2\Big(\frac{1}{2}\dot{D}_a + a\ddot{D}_a\Big) \qquad \dot{D} = \sqrt{a}H_0\dot{D}_a \quad a = \frac{1}{4}H_0\tau^2 \to \tau = 2\frac{\sqrt{a}}{H_0} \tag{A.5}$$

$$H_0^2\Big(\frac{1}{2}\dot{D}_a + a\ddot{D}_a\Big) + \frac{2}{2\sqrt{a}/H_0}\sqrt{a}H_0\dot{D}_a = \frac{6}{4a/H_0^2}D_a \tag{A.6}$$

$$H_0^2\Big(\frac{1}{2}\dot{D}_a + a\ddot{D}_a\Big) + H_0^2\dot{D}_a = \frac{3}{2a}H_0^2D_a \tag{A.7}$$

$$a^2\ddot{D}_a + \frac{3}{2}H_0^2\dot{D}_a = \frac{3}{2}D_a \tag{A.8}$$

A.2 switch from conformal to scale time for neutrino differential equation

Unlike in eq. (A.5) we are not in Einstein-de Sitter

$$\ddot{\delta}_\nu = -\mathcal{H}\dot{\delta}_\nu^{(1)} + \frac{3}{2}\frac{H_0^2\Omega_M}{a}\delta_{cdm}^{(1)} - k^2 c_s(a)^2\delta_\nu^{(1)} \tag{A.9}$$

$$\frac{\mathrm{d}^2}{\mathrm{d}\tau^2} = a\mathcal{H}\frac{\mathrm{d}}{\mathrm{d}a}\Big(a\mathcal{H}\frac{\mathrm{d}}{\mathrm{d}a}\Big) = a\mathcal{H}\Big(\frac{\mathrm{d}a}{\mathrm{d}a}\mathcal{H}\frac{\mathrm{d}}{\mathrm{d}a} + a(\frac{\mathrm{d}}{\mathrm{d}a}\mathcal{H})\frac{\mathrm{d}}{\mathrm{d}a} + a\mathcal{H}\frac{\mathrm{d}^2}{\mathrm{d}a^2}\Big) \tag{A.10}$$

$$= a\mathcal{H}^2\frac{\mathrm{d}}{\mathrm{d}a} + a^2\mathcal{H}\dot{\mathcal{H}}\frac{\mathrm{d}}{\mathrm{d}a} + a^2\mathcal{H}^2\frac{\mathrm{d}^2}{\mathrm{d}a^2} \tag{A.11}$$

$$= H_0^2\Big(\big(\Omega_M + \Omega_\Lambda a^3\big)\frac{\mathrm{d}}{\mathrm{d}a} + \frac{1}{2}\big(-\Omega_M + 2a^3\Omega_\Lambda\big)\frac{\mathrm{d}}{\mathrm{d}a} + \big(\Omega_M a + \Omega_\Lambda a^4\big)\frac{\mathrm{d}^2}{\mathrm{d}a^2}\Big) \tag{A.12}$$

$$\frac{\mathrm{d}^2}{\mathrm{d}\tau^2} = H_0^2\Big(\big(\frac{1}{2}\Omega_M + 2\Omega_\Lambda a^3\big)\frac{\mathrm{d}}{\mathrm{d}a} + \big(\Omega_M a + \Omega_\Lambda a^4\big)\frac{\mathrm{d}^2}{\mathrm{d}a^2}\Big) \tag{A.13}$$

$$\mathcal{H}\frac{\mathrm{d}}{\mathrm{d}\tau} = a\mathcal{H}^2\frac{\mathrm{d}}{\mathrm{d}a} = H_0^2(\Omega_M + \Omega_\Lambda a^3)\frac{\mathrm{d}}{\mathrm{d}a} \tag{A.14}$$

$$\ddot{\delta}_\nu + \mathcal{H}\dot{\delta}_\nu = H_0^2\big(\frac{3}{2}\Omega_M + 3\Omega_\Lambda a^3\big)\dot{\delta}_{\nu,a} + H_0^2\big(\Omega_M a + \Omega_\Lambda a^4\big)\ddot{\delta}_{\nu,a} \tag{A.15}$$

$$H_0^2\big(\frac{3}{2}\Omega_M + 3\Omega_\Lambda a^3\big)\dot{\delta}_{\nu,a} + H_0^2\big(\Omega_M a + \Omega_\Lambda a^4\big)\ddot{\delta}_{\nu,a} = \frac{3}{2}\frac{H_0^2\Omega_M}{a}\delta_{cdm,a}^{(1)} - k^2 c_s(a)^2\delta_{\nu,a}^{(1)} \tag{A.16}$$

$$\big(\frac{3}{2}\Omega_M + 3\Omega_\Lambda a^3\big)\dot{\delta}_{\nu,a} + H_0^2\big(\Omega_M a + \Omega_\Lambda a^4\big)\ddot{\delta}_{\nu,a} = \frac{3}{2}\frac{\Omega_M}{a}\delta_{cdm,a}^{(1)} - \frac{k^2 c_s(a)^2}{H_0^2}\delta_{\nu,a}^{(1)} \tag{A.17}$$

A.3 second order neutrino density perturbation derivations

This section is a simplified summary of how far we got with our approach to $\delta_\nu^{(2)}$.

$$\dot{\delta}^{(1)} = -\theta^{(1)} \quad \dot{\theta}^{(1)} = -\mathcal{H}\theta^{(1)} - \frac{3}{2}\frac{H_0^2\Omega_M}{a}\delta_M^{(1)} - c_s^2\nabla^2\delta^{(1)} \tag{A.18}$$

$$\dot{\delta}_\nu^{(2)} = -2\partial_j\nabla^{-2}\theta^{(1)}\partial_j\delta^{(1)} - 2\delta^{(1)}\theta^{(1)} - \theta^{(2)} \tag{A.19}$$

$$\dot{\theta}^{(2)} = -\mathcal{H}\theta^{(2)} - 2\Big(\partial_i\partial_j\nabla^{-2}\theta^{(1)}\partial_i\partial_j\theta^{(1)}\Big) - 2\partial_j\nabla^{-2}\theta^{(1)}\partial_j\theta^{(1)} - \frac{3}{2}\frac{H_0^2\Omega_M}{a}\delta_M^{(2)} - c_s^2\nabla^2\delta^{(2)} \tag{A.20}$$

$$\ddot{\delta}^{(2)} = -2\partial_j\nabla^{-2}\theta^{(1)}\partial_j\delta^{(1)} - 2\partial_j\nabla^{-2}\dot{\theta}^{(1)}\partial_j\dot{\delta}^{(1)} - 2\dot{\delta}^{(1)}\theta^{(1)} - 2\delta^{(1)}\dot{\theta}^{(1)} - \dot{\theta}^{(2)} \tag{A.21}$$

$$\ddot{\delta}^{(2)} = -2\partial_j\nabla^{-2}\theta^{(1)}\partial_j\delta^{(1)} - 2\partial_j\nabla^{-2}\dot{\theta}^{(1)}\partial_j\dot{\delta}^{(1)} - 2\dot{\delta}^{(1)}\theta^{(1)} - 2\delta^{(1)}\dot{\theta}^{(1)} + \frac{3}{2}\frac{H_0^2\Omega_M}{a}\delta_M^{(2)} + c_s^2\nabla^2\delta^{(2)} + 2\Big(\partial_i\partial_j\nabla^{-2}\theta^{(1)}\partial_i\partial_j\theta^{(1)}\Big) + 2\partial_j\nabla^{-2}\theta^{(1)}\partial_j\theta^{(1)} + \mathcal{H}\theta^{(2)} \tag{A.22}$$

$$\ddot{\delta}^{(2)} = -2\partial_j\nabla^{-2}\theta^{(1)}\partial_j\delta^{(1)} - 2\partial_j\nabla^{-2}\dot{\theta}^{(1)}\partial_j\dot{\delta}^{(1)} - 2\dot{\delta}^{(1)}\theta^{(1)} - 2\delta^{(1)}\dot{\theta}^{(1)} + \frac{3}{2}\frac{H_0^2\Omega_M}{a}\delta_M^{(2)} + c_s^2\nabla^2\delta^{(2)} + 2\Big(\partial_i\partial_j\nabla^{-2}\theta^{(1)}\partial_i\partial_j\theta^{(1)}\Big) + 2\partial_j\nabla^{-2}\theta^{(1)}\partial_j\theta^{(1)} + \mathcal{H}(-2\partial_j\nabla^{-2}\theta^{(1)}\partial_j\delta^{(1)} - 2\delta^{(1)}\theta^{(1)} - \dot{\delta}_v^{(2)}) \tag{A.23}$$

$$\ddot{\delta}^{(2)} = 2\partial_j\nabla^{-2}\delta^{(1)}\partial_j\delta^{(1)} + 2\partial_j\nabla^{-2}(\mathcal{H}\delta^{(1)} - \frac{3}{2}\frac{H_0^2\Omega_M}{a}\delta_M^{(1)} - c_s^2\nabla^2\delta^{(1)})^{(1)}\partial_j\dot{\delta}^{(1)} + 2\dot{\delta}^{(1)}\dot{\delta}^{(1)} - 2\delta^{(1)}(\mathcal{H}\delta^{(1)} - \frac{3}{2}\frac{H_0^2\Omega_M}{a}\delta_M^{(1)} - c_s^2\nabla^2\delta^{(1)}) + \frac{3}{2}\frac{H_0^2\Omega_M}{a}\delta_M^{(2)} + c_s^2\nabla^2\delta^{(2)} + 2\Big(\partial_i\partial_j\nabla^{-2}\dot{\delta}^{(1)}\partial_i\partial_j\dot{\delta}^{(1)}\Big) + 2\partial_j\nabla^{-2}\dot{\delta}^{(1)}\partial_j\dot{\delta}^{(1)} + \mathcal{H}(2\partial_j\nabla^{-2}\dot{\delta}^{(1)}\partial_j\delta^{(1)} + 2\delta^{(1)}\dot{\delta}^{(1)} - \dot{\delta}^{(2)}) \tag{A.24}$$

$$\ddot{\delta}^{(2)} + \mathcal{H}\dot{\delta}^{(2)} = \frac{3}{2}\frac{H_0^2}{a}\Big(2\partial_j\nabla^{-2}\delta_M^{(1)}\partial_j\delta^{(1)} + 2\delta^{(1)}\delta_M^{(1)} + \delta_M^{(2)}\Big) + c_s^2\Big(2\partial_j\delta^{(1)}\partial_j\delta^{(1)} + 2\delta^{(1)}\nabla^2\delta^{(1)} + \nabla^2\delta^{(2)}\Big) 4\partial_j\nabla^{-2}\dot{\delta}^{(1)}\partial_j\dot{\delta}^{(1)} + 2\dot{\delta}^{(1)}\dot{\delta}^{(1)} + 2\partial_i\partial_j\nabla^{-2}\dot{\delta}^{(1)}\partial_i\partial_j\nabla^{-2}\dot{\delta}^{(1)} \tag{A.25}$$